AWARD NUMBER: W81XWH-14-1-0120

TITLE: Temporal Changes in FLT3-ITD Regulation of Stem Cell Self-Renewal and Leukemogenesis

PRINCIPAL INVESTIGATOR: Jeffrey Magee

CONTRACTING ORGANIZATION: Washington University
ST. Louis, MO 63110

REPORT DATE: November 2016

TYPE OF REPORT: Final report

PREPARED FOR: U.S. Army Medical Research and Materiel Command
Fort Detrick, Maryland 21702-5012

REPORT DOCUMENTATION PAGE

Form Approved
OMB No. 0704-0188

1. REPORT DATE	2. REPORT TYPE	3. DATES COVERED
November 2016	Final	1 Sept 2014 – 31 Aug 2016

4. TITLE AND SUBTITLE

Temporal Changes in FLT3-ITD Regulation of Stem Cell Self-Renewal and Leukemogenesis

5a. CONTRACT NUMBER
W81XWH-14-1-0120

5b. GRANT NUMBER
W81XWH-14-1-0120

5c. PROGRAM ELEMENT NUMBER

6. AUTHOR(S)
Dr. Jeffrey Magee

E-Mail: magee_j@kids.wustl.edu

5d. PROJECT NUMBER

5e. TASK NUMBER

5f. WORK UNIT NUMBER

7. PERFORMING ORGANIZATION NAME(S) AND ADDRESS(ES)
Washington University
ST. Louis, MO 63110

8. PERFORMING ORGANIZATION REPORT NUMBER

9. SPONSORING / MONITORING AGENCY NAME(S) AND ADDRESS(ES)

U.S. Army Medical Research and Materiel Command
Fort Detrick, Maryland 21702-5012

10. SPONSOR/MONITOR'S ACRONYM(S)

11. SPONSOR/MONITOR'S REPORT NUMBER(S)

12. DISTRIBUTION / AVAILABILITY STATEMENT

Approved for Public Release; Distribution Unlimited

13. SUPPLEMENTARY NOTES

14. ABSTRACT
My goal is to understand how mechanisms that regulate normal hematopoietic development can also influence the mutation spectra of pediatric and adult acute myeloid leukemia (AML). Genetic differences between pediatric and adult AML may underlie differences in outcomes and necessitate different treatment strategies, yet we have few insights into why these differences occur. To address this problem, we are testing whether one mutation, FLT3-ITD, differentially regulates fetal and adult progenitors. FLT3-ITD mutations are more common in adult AML than in childhood AML, and our studies to date have shown that it has age-specific phenotypes. In adult mice, FLT3-ITD depleted the hematopoietic stem cell (HSC) pool and expanded myeloid progenitor populations. These phenotypes were not evident in fetal mice, even in the presence of a collaborating *Runx1* mutation. To understand why fetal and adult progenitors responded differently to FLT3-ITD, we characterized signal transduction (e.g. STAT5 and MAPK pathways) in fetal, neonatal and adult progenitors. STAT5 was activated by FLT3-ITD at all stages of development, but MAPK was activated only in post-natal progenitors. Furthermore, STAT5 target gene regulation changed through the course of development. We are now testing whether reactivation of fetal gene products can suppress leukemogenesis. Reprogramming therapies may offer a novel approach for treating AML.

15. SUBJECT TERMS
FLT3-ITD, leukemia, hematopoietic stem cell

16. SECURITY CLASSIFICATION OF:			17. LIMITATION OF ABSTRACT	18. NUMBER OF PAGES	19a. NAME OF RESPONSIBLE PERSON
a. REPORT	b. ABSTRACT	c. THIS PAGE			USAMRMC
Unclassified	Unclassified	Unclassified	Unclassified	76	19b. TELEPHONE NUMBER *(include area code)*

Standard Form 298 (Rev. 8-98)
Prescribed by ANSI Std. Z39.18

Table of Contents

Page

2016 FINAL REPORT – JEFFREY A. MAGEE, M.D., Ph.D.

1. INTRODUCTION

The goal of this project is to understand why FLT3-Internal Tandem Duplication (*FLT3-ITD*) mutations cause acute myeloid leukemia (AML) more frequently in adults than in children. *FLT3-ITD* encodes a constitutively active FLT3 tyrosine kinase. This mutation occurs in ~30% of adult AML, but only 5-10% of pediatric AML and <1% of infant AML. This suggests that the mutation preferentially transforms older progenitors. To test whether FLT3-ITD has age-specific effects on hematopoietic stem cells (HSCs) and other hematopoietic progenitors, we characterized its function in fetal, neonatal and adult mouse HSCs. We discovered that FLT3-ITD selectively alters the fate of adult, but not fetal progenitors, primarily due to normal temporal changes in transcriptional regulation that make adult progenitors competent to express FLT3-ITD target genes.

2. KEYWORDS

- Flt3-Internal Tandem Duplication (FLT3-ITD)
- Hematopoietic stem cell (HSC)
- Acute myeloid leukemia
- Stat5
- MAP-kinase

3. ACCOMPLISHMENTS

Major goals:

Aim 1: To test whether *FLT3-ITD* depletes HSCs, expands restricted progenitors and promotes a myeloproliferative neoplasm during the adult, but not fetal stage of development.

Aim 2: To test whether fetal and adult hematopoietic progenitors have different FLT3-ITD driven signal transduction mechanisms and gene expression.

Aim 3: To test whether ectopic *Lin28b* expression impedes FLT3-ITD driven HSC depletion and leukemogenesis.

Accomplishments under these goals:

Aim 1: To test whether FLT3-ITD depletes HSCs, expands restricted progenitors and promotes a myeloproliferative neoplasm during the adult, but not fetal stage of development.

We completed all of the proposed experiments, and the data are incorporated into a manuscript that was just accepted for publication at eLife (acceptance date 11/21/2016). Please see attached manuscript.

Aim 2: To test whether fetal and adult hematopoietic progenitors have different FLT3-ITD driven signal transduction mechanisms and gene expression.

We completed all of the proposed experiments, and the data are incorporated into a manuscript that was just accepted for publication at eLife (acceptance date 11/21/2016). Please see attached manuscript.

<u>Aim 3:</u> To test whether ectopic Lin28b expression impedes FLT3-ITD driven HSC depletion and leukemogenesis.

We have completed all of the proposed experiments. Ectopic Lin28b expression did not prevent Flt3-ITD driven HSC depletion or leukemogenesis. We are now evaluating other fetal gene products, and we are dissecting the gene regulatory networks that make adult hematopoietic progenitors sensitive to FLT3-ITD.

Opportunities for training and professional development:

This work was selected for an oral presentation at the American Society of Hematology annual meeting (December 2015), and it has formed the basis for an R01 proposal that just received a 5th percentile score (final council review pending). Thus, the work supported by CDMRP has opened new lines of investigation, and funding opportunities, that will sustain my lab for years to come. I received guidance from my primary mentor, Sean Morrison, throughout the funding period.

Dissemination of results to communities of interest:

This work has been presented in oral presentations at the International Society for Stem Cell Research Annual meeting and the American Society of Hematology annual meeting. As noted above, an manuscript describing our results has just been accepted at eLife.

Plans for the next reporting period to accomplish the goals:

Nothing to report.

4. IMPACT

Impact on the development of the principal discipline of the project:

This project provides the first evidence that leukemia causing mutations can have age-specific effects on blood forming stem cells and other immature blood cells. This likely contributes to the differences between pediatric and adult leukemias, and It raises the possibility of targeting developmental programs to suppress leukemogenesis.

Impact on other disciplines:

Nothing to report.

Impact on technology transfer:

Nothing to report.

Impact on society beyond science and technology:

Nothing to report.

5. CHANGES/PROBLEMS:

Changes in approach/reasons:

Nothing to report.

Actual or anticipated problems or delays and actions or plans to resolve them:

Nothing to report.

Changes that had a significant impact on expenditures:

Nothing to report.

Significant changes in the use or care of human subjects:

Nothing to report.

Significant changes in the use or care of vertebrate animals:

Nothing to report.

Significant changes in the use of biohazards and/or select agents:

Nothing to report.

6. PRODUCTS

Publications:

Portern SN, Cluster AS, Yang W, Busken KA, Patel RM, Ryoo J, Magee JA. Fetal and neonatal hematopoietic progenitors are functionally and transcriptionally resistant to Flt3-ITD mutations. *eLife* [in press].

Books or one-time publications:

Nothing to report.

Other publications:

Nothing to report.

Websites:

Nothing to report.

Technologies and techniques:

Nothing to report.

Inventions, patent applications or licenses:

Nothing to report.

Other products:

Nothing to report.

7. PARTICIPANTS & OTHER COLLABORATING ORGANIZATIONS

Individuals who have worked on this project:

Name:	Jeffrey Magee, M.D., Ph.D.
Project role	PI
Nearest person month worked	7.2
Contribution to Project	Dr. Magee oversaw the entire research effort including the design, conduct and interpretation of experiments. He also performs experiments.
Funding Support - besides DOD	St. Baldrick's Foundation, Hyundai Hope on Wheels, Gabrielle's Angel Foundation

Name:	Shaina Porter, Ph.D.
Project role	Post-doctoral fellow
Nearest person month worked	12
Contribution to Project	Dr. Porter designed, conducted and interprets experiments under the guidance of the PI. She has conducted the experiments related to temporal changes in FLT3-ITD regulation of HSCs and the signal transduction and gene expression studies.
Funding Support -	Hyundai Hope on Wheels

besides DOD	

Name:	Andrew Cluster, M.D.
Project role	Clinical fellow
Nearest person month worked	4
Contribution to Project	Dr. Cluster characterized the FLT3-ITD; Runx1 compound mutant
Funding Support - besides DOD	Departmental support for clinical trainees – graduate medical education support.

Name:	Jenna Voigtmann
Project role	Research technician
Nearest person month worked	6
Contribution to Project	Ms. Voigtmann managed the mouse colony and assisted with experiments.
Funding Support - besides DOD	St. Baldrick's Foundation and institutional funds.

Name:	Kelsey Busken
Project role	Research technician
Nearest person month worked	6
Contribution to Project	Ms. Busken managed the mouse colony and assisted with experiments.
Funding Support - besides DOD	Hyundai Hope on Wheels, St. Baldrick's Foundation

Name:	Riddhi Patel
Project role	Research technician
Nearest person month worked	6
Contribution to Project	Ms. Patel co-managed the mouse colony and assisted with experiments.
Funding Support - besides DOD	Hyundai Hope on Wheels, St. Baldrick's Foundation

Name:	Wei Yang
Project role	Bioinformaticist
Nearest person month worked	0.5
Contribution to Project	Dr. Wang performed all of the computational work associated with this project – e.g. microarray analyses.
Funding Support - besides DOD	No grant support – supported by the department of biostatistics

Name:	Jiyeon Ryoo
Project role	Research technician
Nearest person month worked	4
Contribution to Project	Ms. Ryoo co-managed the mouse colony and assisted with experiments.
Funding Support - besides DOD	Hyundai Hope on Wheels, St. Baldrick's Foundation

Changes in active other support of the PD/PUI or senior key personnel:

Nothing to report.

Other organizations that were involved as partners:

Nothing to report.

8. SPECIAL REPORTING REQUIREMENTS

Nothing to report.

9. APPENDICES

Please see attached manuscript

Fetal and neonatal hematopoietic progenitors are functionally and transcriptionally resistant to *Flt3*-ITD mutations

Shaina N. Porter[1], Andrew S. Cluster[1], Wei Yang[2], Kelsey A. Busken[1], Riddhi M. Patel[1], Jiyeon Ryoo[1], Jeffrey A. Magee[1, 2, 3]

1. Division of Pediatric Hematology and Oncology, Department of Pediatrics, Washington University School of Medicine, St. Louis, MO, 63110, USA

2. Department of Genetics, Washington University School of Medicine, St. Louis, MO, 63110, USA

3. Corresponding author
Department of Pediatrics
Washington University School of Medicine
660 S. Euclid Ave, Box 8220
St. Louis, MO 63110

Abstract

The *FLT3* Internal Tandem Duplication (*FLT3*^{ITD}) mutation is common in adult acute myeloid leukemia (AML) but rare in early childhood AML. It is not clear why this difference occurs. Here we show that *Flt3*^{ITD} and cooperating *Flt3*^{ITD}*/Runx1* mutations cause hematopoietic stem cell depletion and myeloid progenitor expansion during adult but not fetal stages of murine development. In adult progenitors, FLT3^{ITD} simultaneously induces self-renewal and myeloid commitment programs via STAT5-dependent and STAT5-independent mechanisms, respectively. While FLT3^{ITD} can activate STAT5 signal transduction prior to birth, this signaling does not alter gene expression until hematopoietic progenitors transition from fetal to adult transcriptional states. Cooperative interactions between *Flt3*^{ITD} and *Runx1* mutations are also blunted in fetal/neonatal progenitors. Fetal/neonatal progenitors may therefore be protected from leukemic transformation because they are not competent to express FLT3^{ITD} target genes. Changes in the transcriptional states of developing hematopoietic progenitors may generally shape the mutation spectra of human leukemias.

Introduction

Acute myeloid leukemia (AML) can occur at any stage of life yet the mutations that cause AML differ between childhood and adulthood, especially when one compares young children to adults (Chaudhury et al., 2015). For example, *MLL* translocations and *GATA1* mutations are common in infant and early childhood AML but rare in adult AML (Andersson et al., 2015; Horton et al., 2013; Pine et al., 2007). Mutations in *FLT3*, *NPM1*, *DNMT3A*, *TET2* and *IDH1* are all common in adult AML but rare in infant and early childhood AML (Cancer Genome Atlas Research Network, 2013; Ho et al., 2011; Liang et al., 2013; Zwaan et al., 2003). The genetic differences between pediatric and adult AML are not absolute, but they reflect a more general phenomenon in leukemia biology – leukemias in infants, young children, older children and adults have different genetic and epigenetic landscapes, different mechanisms of transformation and different clinical courses (Downing and Shannon, 2002). Efforts to interpret AML genomes and translate the information into useful therapies will need to account for the influences of age and developmental context on leukemia cell biology. This will require a better understanding of how normal developmental programs shape the process of leukemogenesis.

The mutations that cause AML are thought to accrue first in pre-leukemic hematopoietic stem cells (HSCs) or committed hematopoietic progenitor cells (HPCs) (Jan et al., 2012; Welch et al., 2012), and several properties of these cells change between fetal and adult stages of life: 1) Fetal HSCs divide frequently and retain their self-renewal capacity through cumulative division

cycles (Pietras and Passegue, 2013). In contrast, adult HSCs are usually quiescent, and self-renewal capacity declines with cumulative divisions (Foudi et al., 2009; Pietras and Passegue, 2013; Wilson et al., 2008). 2) Fetal and adult HSCs have distinct self-renewal mechanisms. For example, *Sox17* is required for fetal, but not adult, HSC self-renewal (Kim et al., 2007). *Etv6*, *Ash1l, Mll* and *Pten* are all required for adult, but not fetal, HSC self-renewal (Hock et al., 2004; Jones et al., 2015; Jude et al., 2007; Magee et al., 2012). 3) Fetal and adult HSCs give rise to committed progenitors with distinct epigenetic landscapes (Huang et al., 2016; Xu et al., 2012) and distinct lineage biases (Benz et al., 2012; Copley et al., 2013; Yuan et al., 2012). These observations raise the question of whether mutations can have age-specific effects on gene expression, self-renewal, differentiation and ultimately leukemogenesis. If so, competence for transformation may be a heterochronic property of HSCs and HPCs, and this may explain why pediatric and adult leukemias have different mutations.

The *FLT3 Internal Tandem Duplication* (*FLT3*^{ITD}) is an example of an AML driver mutation that occurs more commonly in adults than in young children (30-40% of adult AML, 5-10% of AML in children <10 years old, <1% of infant AML) (Meshinchi et al., 2006). *FLT3*^{ITD} encodes a constitutively active tyrosine kinase receptor that has been shown to activate the STAT5, MAP-kinase (MAPK), PI3-kinase (PI3K), STAT3 and NF-κB signal transduction pathways in various contexts (Choudhary et al., 2007; Gerloff et al., 2015; Radomska et al., 2006). Mice with a targeted *Flt3*^{ITD} mutation develop myeloproliferative neoplasms (MPN) (Lee et al., 2007; Li et al., 2008), and several other mutations (e.g. *Npm1*,

93 *Tet2* and *Runx1* mutations) cooperate with *Flt3*^{ITD} to drive AML in mice much as
94 in humans (Mead et al., 2013; Mupo et al., 2013; Rau et al., 2014; Shih et al.,
95 2015). In the absence of cooperating mutations, *Flt3*^{ITD} drives adult HSCs into
96 cycle and depletes the HSC pool (Chu et al., 2012). This may explain why
97 *FLT3*^{ITD} mutations occur late in the clonal evolution of human AML – adult HSCs
98 must first acquire mutations that preserve (or ectopically establish) self-renewal
99 capacity in pre-leukemic progenitors – but it also raises the question of why
100 fetal/neonatal HSCs, which have an inherently high self-renewal capacity (He et
101 al., 2009), do not give rise to *FLT3*^{ITD} positive AML more often than is observed.
102 To better understand how developmental context shapes myeloid
103 leukemogenesis, we characterized the effects of *Flt3*^{ITD} on HSC self-renewal,
104 myelopoiesis, signal transduction and gene expression at several stages of pre-
105 and post-natal development. *Flt3*^{ITD} did not cause HSC depletion or myeloid
106 progenitor expansion until after birth. This was true even in the presence of a
107 cooperating *Runx1* loss-of-function mutation. The FLT3^{ITD} protein phosphorylated
108 STAT5 during both pre- and post-natal stages of development while it hyper-
109 activated the MAPK pathway only after birth. To our surprise, MAPK inhibition
110 failed to rescue HSC depletion and myeloid progenitor expansion in adult *Flt3*^{ITD}
111 mice, and *Stat5a/b* deletion greatly exacerbated these phenotypes. FLT3^{ITD}
112 target genes, including STAT5 targets, were not induced in fetal HSCs or HPCs
113 despite pre-natal STAT5 phosphorylation. Instead, FLT3^{ITD} target gene activation
114 coincided with a normal transition from fetal to adult gene expression that was

evident by two weeks after birth. These temporal changes in FLT3^{ITD} target gene expression were observed even in the setting of a cooperating *Runx1* mutation.

Our data establish a crucial role for developmental context in the pathogenesis of *FLT3^{ITD}*-driven AML. Fetal and neonatal progenitors are protected from transformation because they are not competent to express FLT3^{ITD} target genes. This likely explains why *FLT3^{ITD}* mutations are more common in adults than young children, and it may reflect a more general role for developmental programming in leukemia pathogenesis.

Results

Flt3^{ITD} does not deplete fetal HSCs

Since *FLT3^{ITD}* occurs more commonly in adult AML patients than in young children, we hypothesized that it might have age-specific effects on self-renewal and myelopoiesis. We first tested whether *Flt3* expression changes with age. We measured *Flt3* transcript expression in CD150^{+}CD48^{-}Lineage^{-}Sca1^{+}c-kit^{+} HSCs and CD48^{+}Lineage^{-}Sca1^{+}c-kit^{+} HPCs from 8-10 week old adult and embryonic day (E)14.5 fetal mice by quantitative RT-PCR (qRT-PCR). *Flt3* was more highly expressed in HPCs than in HSCs at both ages (Fig. 1A), consistent with prior studies (Buza-Vidas et al., 2011), but its expression did not change with age in either cell population (Fig. 1A). Flow cytometry confirmed that the FLT3 protein is expressed in both fetal and adult progenitors (Fig. 1B).

Since *Flt3^{ITD}* has previously been shown to deplete adult HSCs (Chu et al., 2012), we tested whether the mutation has a similar effect on fetal HSC

numbers. We measured HSC numbers in 8-10 week old adult bone marrow and E14.5 fetal livers from wild type, *Flt3*$^{ITD/+}$ and *Flt3*$^{ITD/ITD}$ mice. Adult *Flt3*$^{ITD/+}$ mice had ~50% fewer HSCs than wild type littermates, consistent with prior studies, and *Flt3*$^{ITD/ITD}$ mice had a near-complete loss of phenotypic HSCs (Fig. 1C). HSC depletion in the bone marrow was not accompanied by extramedullary expansion of HSCs in the spleen (Fig. 1E), in contrast to other leukemogenic mutations (e.g. *Pten* deletion) that cause depletion of bone marrow HSCs but marked expansion of the spleen HSC population (Magee et al., 2012; Porter et al., 2016). Unlike adult mice, *Flt3*$^{ITD/+}$ and *Flt3*$^{ITD/ITD}$ fetal mice had similar numbers of HSCs as wild type littermates (Fig. 1D). The *Flt3*^{ITD} mutation therefore depletes adult, but not fetal HSCs.

We next tested whether fetal *Flt3*$^{ITD/ITD}$ HSCs are functionally impaired. We performed limiting dilution transplantation assays with either 8-10 week old adult bone marrow cells (600,000, 100,000, 50,000 or 10,000 CD45.2 donor cells competed with 300,000 CD45.1 adult bone marrow cells) or E14.5 fetal liver cells (100,000, 50,000 or 10,000 CD45.2 donor cells competed with 300,000 CD45.1 adult bone marrow cells). Two independent experiments were performed, and fetal and adult donor cells were transplanted at the same time in each experiment. Multi-lineage reconstitution was assessed every 4 weeks for 16 weeks following the transplants, and functional HSC frequencies were calculated by Extreme Limiting Dilution Analysis (Hu and Smyth, 2009). Adult *Flt3*$^{ITD/ITD}$ bone marrow had significantly fewer functional HSCs than adult wild type bone marrow

(P<0.00001, Fig. 1F). In contrast, wild type and *Flt3*$^{ITD/ITD}$ fetal livers had similar HSC frequencies (Fig. 1G).

Our findings raised the question of whether fetal *Flt3*$^{ITD/ITD}$ HSCs can mature and become depleted after transplantation into adult recipient mice. To test this, we measured donor HSC chimerism in primary recipients of 100,000 wild type and *Flt3*$^{ITD/ITD}$ fetal liver cells (from Figure 1G). Donor *Flt3*$^{ITD/ITD}$ HSCs were significantly depleted in primary recipient mice, but wild type competitor HSCs were not (Fig. 1H). Overall donor bone marrow chimerism was not significantly different between recipients of wild type and *Flt3*$^{ITD/ITD}$ fetal liver cells (Fig. 1I). Secondary transplants confirmed depletion of *Flt3*$^{ITD/ITD}$ HSCs in the marrow of primary recipients (Fig. 1J, K). Thus, fetal *Flt3*$^{ITD/ITD}$ HSCs are functional, but they lose repopulating activity after transplantation into adult recipient mice.

Flt3^{ITD} *causes HSC depletion and myeloid progenitor expansion by 2 weeks after birth in mice*

We next sought to define the age at which *Flt3*^{ITD} begins to deplete HSCs and expand myeloid progenitor populations. We measured HSCs, HPCs and granulocyte-monocyte progenitor (GMP) numbers at E14.5, E16.5, post-natal day (P)0 and P14. *Flt3*$^{ITD/+}$ and *Flt3*$^{ITD/ITD}$ mice had normal HSC numbers at all ages prior to birth (Fig. 2A). HSC depletion was evident at P14 in both the bone marrow and the spleen, though not to the extent observed in adult bone marrow (Fig. 2B). We observed a modest increase in *Flt3*$^{ITD/+}$ and *Flt3*$^{ITD/ITD}$ HPCs and

GMPs at P0 (Fig. 2C, E), and this phenotype became more severe, particularly in *Flt3*$^{ITD/ITD}$ mice, by P14 (Fig. 2D, E). Spleen enlargement due to MPN was evident by P14 in *Flt3*$^{ITD/+}$ and *Flt3*$^{ITD/ITD}$ mice, but E14.5, E16.5 and P0 liver sizes were not increased relative to wild type littermates (Fig. 2F). These data show that *Flt3*^{ITD} causes HSC depletion, HPC/GMP expansion and MPN beginning at or shortly after birth.

FLT3^{ITD} mutations usually occur late during the clonal evolution of human AML. This raises the question of whether fetal/neonatal *Flt3*^{ITD} mice can exhibit HSC depletion and HPC/GMP expansion when a cooperating mutation is present. To test this, we analyzed HSC, HPC and GMP frequencies in *Flt3*$^{ITD/+}$*; Runx1*$^{f/+}$*; Vav1-Cre* mice. Both mono- and bi-allelic *RUNX1* loss-of-function mutations co-occur with *FLT3*^{ITD} in human AML (Schnittger et al., 2011), and *Runx1* deletions synergize with *Flt3*^{ITD} to cause AML in mice (Mead et al., 2013). For the purposes of these studies we focused on mono-allelic *Runx1* deletions because bi-allelic deletions severely depleted phenotypic HSCs irrespective of the *Flt3* genotype (data not shown). These effects were likely due to previously described, *Runx1*-dependent changes in CD48 expression (Cai et al., 2011).

We evaluated HSC, HPC and GMP frequencies in 1) *Flt3*$^{+/+}$*; Runx1*$^{f/f}$ or *Runx1*$^{f/+}$*; Cre*-negative (control), 2) *Flt3*$^{ITD/+}$*; Runx1*$^{f/f}$ or *Runx1*$^{f/+}$*; Cre*-negative (*Flt3*$^{ITD/+}$), 3) *Flt3*$^{+/+}$*;Runx1*$^{f/+}$*; Vav1-Cre* (*Runx1*$^{\Delta/+}$) and 4) *Flt3*$^{ITD/+}$*;Runx1*$^{f/+}$*; Vav1-Cre* (*Flt3*$^{ITD/+;}$ *Runx1*$^{\Delta/+}$) littermates at E14.5, P0, P14 and P21. HSCs were severely depleted in P14 and P21 *Flt3*$^{ITD/+;}$ *Runx1*$^{\Delta/+}$ mice relative to controls and single mutant mice (Fig. 3C, D). In contrast, all four genotypes of mice had

206 similar HSC frequencies at P0 (Fig. 3B), and *Runx1* heterozygosity increased
207 HSC frequency at E14.5 irrespective of the *Flt3* genotype (Fig. 3A). HPCs and
208 GMPs were markedly expanded in P14 and P21 $Flt3^{ITD/+;}$ $Runx1^{\Delta/+}$ mice (Fig. 3G,
209 H, K, L). These populations were only modestly expanded in compound mutant
210 mice at P0 (Fig. 3F, J), and they were not expanded at all at E14.5 (Fig. 3E, I).
211 We next tested whether compound $Flt3^{ITD}$ and *Runx1* mutations had age-
212 specific effects on HSC/HPC function. We transplanted 100,000 P0 liver cells or
213 P21 bone marrow cells from control or $Flt3^{ITD/+;}$ $Runx1^{\Delta/+}$ littermate donors, along
214 with 300,000 wild type competitor cells, into irradiated CD45.1 recipient mice. At
215 2 weeks after the transplants, we observed $CD45.2^{+}$ donor-derived leukocytes in
216 the peripheral blood of all recipients, irrespective of donor age or genotype (Fig.
217 3M, N). At 4 weeks after the transplants, donor chimerism was significantly and
218 dramatically reduced in recipients of $Flt3^{ITD/+;}$ $Runx1^{\Delta/+}$ P21 donor cells as
219 compared to recipients of control P21 donor cells and $Flt3^{ITD/+;}$ $Runx1^{\Delta/+}$ P0 donor
220 cells (Fig. 3M). Indeed, only 1 of 15 recipients of $Flt3^{ITD/+;}$ $Runx1^{\Delta/+}$ P21 donor
221 cells had multi-lineage donor chimerism (>0.5% $CD45.2^{+}$ myeloid and lymphoid
222 cells) (Fig. 3O). In contrast, all recipients of control and $Flt3^{ITD/+;}$ $Runx1^{\Delta/+}$ P0
223 donor cells had multi-lineage donor chimerism (Fig. 3O). These differences were
224 evident even when we focused specifically on myeloid chimerism (Fig. 3N, P), so
225 they were not simply a reflection of altered lineage biases in the $Flt3^{ITD/+;}$
226 $Runx1^{\Delta/+}$ progenitors. Altogether, these data show that $Flt3^{ITD}$ has developmental
227 context-specific effects on HSC depletion, myeloid progenitor expansion and
228 repopulating activity, even when paired with a cooperating *Runx1* mutation.

Flt3^{ITD} activates STAT5 and MAPK signal transduction pathways in adult HSCs and HPCs, yet it only activates STAT5 in fetal HSCs

To better understand why *Flt3^{ITD}* has developmental context-specific effects on HSCs and HPCs, we sought to better characterize the pathways that mediate FLT3^{ITD} signal transduction *in vivo*. We isolated 25,000 HSC/multipotent progenitors (HSC/MPPs; CD48^{-}Lineage^{-}Sca1^{+}c-kit^{+}), HPCs and GMPs from adult mice by flow cytometry, and we performed Western blots to assess phosphorylation of STAT5, STAT3, ERK1/2 (a MAPK pathway protein) and AKT (a PI3K pathway protein). Both STAT5 and ERK1/2 were hyper-phosphorylated in *Flt3^{ITD}* HSC/MPPs and HPCs, as well as in adult *Flt3^{ITD}; Runx1$^{\Delta/\Delta}$* AML cells (Fig. 4A-C). In contrast, STAT3 and AKT were not hyper-phosphorylated in *Flt3^{ITD}* mutant HSC/MPPs or HPCs (Fig. 4A and Fig. 4 – figure supplement 1A), and *Rictor* deletion (PI3K/mTORC2 pathway inactivation) did not rescue *Flt3^{ITD}*-driven HSC depletion or MPN (Fig. 4 – figure supplement 1B, C). These findings suggest that the STAT5 and MAPK pathways mediate FLT3^{ITD} signal transduction in hematopoietic progenitors, but the STAT3 and PI3K pathways do not.

We next tested whether FLT3^{ITD} signal transduction changes between fetal and adult stages of development. We isolated HSC/MPPs and HPCs from wild type and *Flt3^{ITD}* mice at E14.5, P0, P14 and 8 weeks after birth. We performed Western blots to assess STAT5 and ERK1/2 phosphorylation. STAT5 was hyper-phosphorylated in *Flt3^{ITD}* mutant HSC/MPPs and HPCs at all stages

252 of development, though the degree of STAT5 phosphorylation appeared to
253 increase with age (Fig. 4D, E). ERK1/2 was only hyper-phosphorylated in post-
254 natal *Flt3*^{ITD} mutant HSC/MPPs and HPCs (Fig. 4D, F). Several other signal
255 transduction proteins, including STAT3, AKT, ribosomal protein S6, p38 and
256 JNK, were not hyper-phosphorylated in *Flt3*^{ITD} HSC/MPPs or HPCs at any age
257 tested, or their phosphorylation was undetectable (data not shown). Our data
258 reinforce other studies that have implicated STAT5 and MAPK as key
259 downstream effectors of FLT3^{ITD} signaling (Choudhary et al., 2007; Radomska et
260 al., 2006). However, the data suggest that these pathways are not coupled –
261 STAT5 is phosphorylated in fetal progenitors without concurrent MAPK pathway
262 activation. This raises the question of whether each pathway has unique
263 functions downstream of FLT3^{ITD}.
264
265 *MAPK pathway inhibition has little to no effect on Flt3*^{ITD}*-driven HSC depletion,*
266 *HPC expansion and GMP expansion.*
267 We used the MEK inhibitor PD0325901 to test whether MAPK pathway
268 inhibition could prevent HSC depletion and HPC/GMP expansion in *Flt3*^{ITD} mice.
269 We administered vehicle or PD0325901 to 6-week-old wild type and *Flt3*$^{ITD/+}$
270 mice (5 mg/kg per day for 10 days). This regimen effectively inhibited ERK1/2
271 phosphorylation in HPCs without affecting STAT5 phosphorylation (Fig. 5 – figure
272 supplement 1). PD0325901-treated wild type mice had significantly more
273 phenotypic HSCs and HPCs than vehicle treated controls (Fig. 5A, B). However,
274 PD0325901 had no effect on HSC numbers, HPC numbers or GMP frequencies

in *Flt3*$^{ITD/+}$ mice (Fig. 5A-C). This suggests that sustained MAPK pathway signaling is not required for HSC depletion, HPC expansion and GMP expansion in *Flt3*$^{ITD/+}$ adult mice.

We next tested whether PD0325901could prevent the onset of the HSC depletion, HPC expansion and GMP expansion phenotypes if it was given shortly after birth. We treated nursing mothers of wild type, *Flt3*$^{ITD/+}$ and *Flt3*$^{ITD/ITD}$ neonates with PD0325901 (5 mg/kg per day) beginning at P1. While this regimen has previously been shown to rescue MAPK pathway-dependent developmental abnormalities in *Nf1* mutant neonates (Wang et al., 2012), it did not prevent HSC depletion or HPC expansion in *Flt3*^{ITD} mutant neonates (Fig. 5D, E), and it only partially rescued GMP expansion (Fig. 5F). Altogether, the data suggest that the MAPK pathway has only a minor role, if any, in causing these phenotypes. Temporal changes in MAPK pathway regulation are unlikely to account for the different effects of FLT3^{ITD} on fetal and adult progenitors.

STAT5 inactivation exacerbates HSC depletion, HPC expansion, GMP expansion and MPN.

STAT5 has been implicated as a key downstream effector of FLT3^{ITD} in many different systems, and it is hyper-phosphorylated in *Flt3*$^{ITD/+}$ HSCs and HPCs during fetal, neonatal and adult stages of development (Fig. 4E, F). This raised the question of whether genetic inactivation of *Stat5a* and *Stat5b* – with a conditional *Stat5a/b* allele (Wang et al., 2009) – could prevent HSC depletion, HPC expansion, GMP expansion and MPN in *Flt3*$^{ITD/+}$ mice. To answer this

question, we evaluated HSCs, HPCs, GMPs and spleen weights in 1) *Flt3*$^{+/+}$; *Stat5a/b*$^{f/+}$ or *Stat5a/b*$^{f/f}$; Cre^{-} (control), 2) *Flt3*$^{+/+}$*; Stat5a/b*$^{f/+}$*; Mx1-Cre* (*Stat5*$^{\Delta/+}$), 3) *Flt3*$^{+/+}$*; Stat5a/b*$^{f/f}$*; Mx1-Cre* (*Stat5*$^{\Delta/\Delta}$), 4) *Flt3*$^{ITD/+}$; *Stat5a/b*$^{f/+}$ or *Stat5a/b*$^{f/f}$; Cre^{-} (*Flt3*$^{ITD/+}$), 5) *Flt3*$^{ITD/+}$*; Stat5a/b*$^{f/f}$*; Mx1-Cre* (*Flt3*^{ITD}*; Stat5*$^{\Delta/+}$), and 6) *Flt3*$^{ITD/+}$*; Stat5a/b*$^{f/f}$*; Mx1-Cre* (*Flt3*$^{ITD/+}$*; Stat5*$^{\Delta/\Delta}$) mice. The mice were treated with poly-inosine:poly-cytosine (pIpC) beginning at 6 weeks after birth to delete *Stat5a/b*, and they were analyzed 4 weeks later. Western blotting confirmed complete loss of STAT5 protein, and MAPK pathway activation was unaffected by *Stat5a/b* deletion (Fig. 6 – figure supplement 1). Surprisingly, *Stat5a/b* deletion exacerbated the HSC depletion, HPC expansion and GMP expansion phenotypes of *Flt3*$^{ITD/+}$ mice rather than rescuing them (Fig. 6A-C). Spleen weights were also enlarged in *Flt3*^{ITD}*; Stat5*$^{\Delta/+}$ and *Flt3*$^{ITD/+}$*; Stat5*$^{\Delta/\Delta}$ mice relative to control, *Stat5*$^{\Delta/+}$, *Stat5*$^{\Delta/\Delta}$ and *Flt3*$^{ITD/+}$ littermates (Fig. 5D). Similar results were observed when we deleted a single *Stat5a/b* with *Vav1-cre*. Only one *Stat5a/b* allele was deleted in these analyses because bi-allelic deletion impairs fetal erythropoiesis (Zhu et al., 2008). Nevertheless, *Flt3*$^{ITD/+}$*; Stat5a/b*$^{f/+}$*; Vav1-Cre* mice had fewer HSCs, more HPCs, more GMPs and larger spleens than control or *Flt3*$^{ITD/+}$ littermates at 8-10 weeks after birth (Fig. 6E-H).

The data reveal an unanticipated function for STAT5 in pre-leukemic, *Flt3*^{ITD}-mutant progenitors. They suggest that STAT5 helps to maintain *Flt3*^{ITD}-mutant HSCs in an uncommitted state and that it antagonizes *Flt3*^{ITD}-driven expansion of more committed myeloid progenitor populations. Thus, FLT3^{ITD} may

simultaneously potentiate self-renewal and myeloid commitment programs via STAT5-dependent and STAT5-independent pathways, respectively (Fig. 6I).

FLT3^{ITD} activates self-renewal programs in HPCs via STAT5, and it activates commitment programs independently of STAT5 The changes in HSC and HPC frequencies in *Flt3^{ITD}; Stat5a/b* compound mutant mice raise the question of whether FLT3^{ITD} has STAT5-dependent and STAT5-independent effects on gene expression, and whether transcriptional changes are developmental context-specific. To answer these questions we performed two independent experiments to characterize global changes in gene expression (Fig. 7A). In the first experiment, we analyzed gene expression in wild type and *Flt3$^{ITD/+}$* HSCs and HPCs at E14.5, P0, P14 and 8-10 weeks after birth. This experiment was meant to elucidate changes in FLT3^{ITD} target genes over time. In the second experiment, we analyzed gene expression in adult HPCs from 1) wild type, 2) *Flt3$^{ITD/+}$,* 3) *Flt3$^{ITD/ITD}$*, 4) *Flt3^{ITD}; Stat5$^{\Delta/+}$* and 5) *Flt3$^{ITD/+}$; Stat5$^{\Delta/\Delta}$* mice. This experiment was meant to delineate which FLT3^{ITD} targets are STAT5-dependent and which are STAT5-independent.

We analyzed the data from each experiment independently, and we merged the data to identify a list of genes that were significantly, differentially expressed in FLT3^{ITD} progenitors in both experiments. In experiment 1, we identified 254 annotated coding genes that were differentially expressed between wild type and *Flt3$^{ITD/+}$* HPCs at one or more time points (Fig. 7 – source data table 1; adjusted $p<0.05$; fold change ≥2). We did not identify any genes that met

these stringent filtering criteria in HSCs, though statistically significant changes in gene expression were observed when specific target genes (from the HPC list) were individually interrogated ($p<0.05$, Fig. 7 – source data table 1). The differences between HSCs and HPCs may simply reflect differences in *Flt3* expression (Fig. 1A), though it is also possible that HSCs with the strongest transcriptional responses to $FLT3^{ITD}$ were not captured in our microarray assays because they differentiated. Of the 254 genes that were differentially expressed in experiment 1, 58 unique genes were also differentially expressed between wild type and $Flt3^{ITD/+}$ HPCs in experiment 2 (Fig. 7B and Fig. 7 – figure supplement 1). Thirty-three genes were expressed at higher levels in $Flt3^{ITD}$ HPCs relative to wild type HPCs, and 25 genes were expressed at lower levels (Fig. 7B). Of these, 35 normalized when *Stat5a/b* was deleted, but 23 did not. $FLT3^{ITD}$ therefore has both STAT5-dependent and STAT5-independent effects on gene expression, and these effects are more pronounced in HPCs as compared to HSCs.

We tested whether $FLT3^{ITD}$ activates self-renewal- and commitment-related transcriptional programs via STAT5-dependent and STAT5-independent mechanisms, respectively, as predicted by our phenotypic assays (Fig. 6). We generated self-renewal-related and commitment-related gene sets by comparing wild type HSCs and HPCs using the data collected in experiment 1 (Figure 7 – source data table 2). We then used Gene Set Enrichment Analysis (GSEA) to compare wild type, $Flt3^{ITD/+}$ and $Flt3^{ITD/+}; Stat5^{\Delta/\Delta}$ HPCs using data collected in experiment 2 (Subramanian et al., 2005). Self-renewal-related genes were

enriched in *Flt3*$^{ITD/+}$ HPCs, and commitment-related genes were enriched in wild type HPCs (Fig. 7C). This suggests that the FLT3^{ITD} protein can activate self-renewal mechanisms in otherwise non-self-renewing HPCs. Remarkably, these effects were strongly reversed when *Stat5a/b* was deleted (Fig. 7C). A separately curated self-renewal gene set from Ivanova et al. was similarly enriched in wild type and *Flt3*$^{ITD/+}$ HPCs as compared to *Flt3*$^{ITD/+}$*; Stat5*$^{\Delta/\Delta}$ HPCs (Fig. 7D) (Ivanova et al., 2002). These findings are consistent with a model in which FLT3^{ITD} signals via STAT5 to ectopically activate self-renewal programs in HPCs, and it simultaneously promotes myeloid commitment via STAT5-independent mechanisms.

To better understand the STAT5-independent mechanisms that promote myeloid commitment, we performed GSEA on *Flt3*$^{ITD/+}$ and *Flt3*$^{ITD/+}$*; Stat5*$^{\Delta/\Delta}$ HPCs with curated gene sets in the MSigDB database (Subramanian et al., 2005). The most significantly enriched gene sets in *Flt3*$^{ITD/+}$*; Stat5*$^{\Delta/\Delta}$ HPCs were generally associated with increased inflammatory cytokine signaling (Fig. 7E). This finding is intriguing because several prior studies have linked inflammatory cytokine signaling to loss of adult HSC self-renewal capacity and myeloid differentiation (Baldridge et al., 2010; Essers et al., 2009; Pietras et al., 2016). Of note, we did not observe changes in STAT1, STAT3 or AKT phosphorylation in *Flt3*$^{ITD/+}$*; Stat5*$^{\Delta/\Delta}$ HPCs (Fig. 6 – figure supplement 1 and data not shown). Additional studies are still needed to identify the signal transduction molecules that mediate FLT3^{ITD}-driven myeloid commitment, and to test whether changes in

cytokine-related gene expression are a cause or a consequence of differentiation in *Flt3*$^{ITD/+}$*; Stat5*$^{\Delta/\Delta}$ HPCs.

FLT3^{ITD}*-mediated changes in gene expression correlate temporally with the normal transition from fetal to adult transcriptional programs*

FLT3^{ITD} has the capacity to activate functionally relevant signal transduction pathways, such as STAT5, during both pre- and post-natal stages of development (Fig. 4), yet HSC and HPC phenotypes were only observed after birth. This raises the question of whether pre- and post-natal progenitors have distinct transcriptional responses to FLT3^{ITD}. We evaluated FLT3^{ITD} target gene expression in HPCs at E14.5, P0, P14 and adulthood (Fig. 8A). We found that differences between wild type and *Flt3*$^{ITD/+}$ HPCs were more evident at P14 and adulthood than at E14.5 or P0 (Fig. 8A and Fig. 8 – figure supplement 1). This was true for both STAT5-dependent targets, e.g. *Socs2*, and STAT5-independent targets, e.g. *Ctsg* (Fig. 8B). Thus, fetal, neonatal and adult hematopoietic progenitors have distinct transcriptional responses to FLT3^{ITD} signaling.

To better understand when HSCs and HPCs transition from fetal to adult transcriptional programs, we analyzed gene expression in wild type cells from experiment 1. We identified 2627 unique genes (from 3005 different probes) that exhibited significant changes in gene expression in HSCs between E14.5 and adulthood. Of the 228 most differentially expressed transcripts (from the top 250 probes), all followed a consistent trend toward increasing (109 genes) or decreasing (119 genes) expression with increasing age, and most were

411 differentially expressed in both HSCs and HPCs (Fig. 8C, Fig. 8 – source data
412 table 1). Among these genes were several that encode transcription factors and
413 RNA binding proteins that are known to regulate HSC self-renewal, including
414 *Lin28b*, *Esr1, Hmga2* and *Egr1* (Fig. 8C, D). Principal component analysis and
415 Euclidean distance measurements showed that P14 HSCs more closely
416 resembled adult HSCs than fetal HSCs, and P0 HSCs more closely resembled
417 fetal HSCs (Fig. 8E). Similar associations were observed for HPCs (Fig. 8 –
418 figure supplement 2). The data show that HSCs and HPCs begin transitioning
419 from fetal to adult transcriptional programs by P14, even before they achieve
420 quiescence (Bowie et al., 2006). Furthermore, the data suggest that HSCs and
421 HPCs become competent to express (or repress) $FLT3^{ITD}$ target genes as they
422 transition from fetal to adult transcriptional programs.
423
424 *$Flt3^{ITD}$ and Runx1 heterozygous mutations collaboratively induce changes in*
425 *gene expression in a developmental context-dependent manner*
426 *$Flt3^{ITD}$* and *Tet2* loss of function mutations have recently been shown to
427 cooperatively induce changes in gene expression and DNA methylation in adult
428 HPCs that are not observed with either mutation alone (Shih et al., 2015). We
429 tested whether *$Flt3^{ITD}$* and *Runx1* mutations have similar cooperative effects on
430 transcription and whether the effects are age-specific. We evaluated gene
431 expression in 1) wild type, 2) *$Runx1^{\Delta/+}$*, 3) *$Flt3^{ITD/+}$* and 4) *$Flt3^{ITD/+}$; $Runx1^{\Delta/+}$* HPCs
432 at P0 and P14. At P14, we identified 191 genes that were significantly
433 differentially expressed between wild type and *$Flt3^{ITD/+}$; $Runx1^{\Delta/+}$* HPCs (adj.

434 p<0.05; fold change ≥3). At P0 only 8 genes met these criteria, 7 of which
435 overlapped with the P14 gene list (Fig. 9A and Fig. 9 – source data table 1).
436 GSEA showed significant overlap between genes that were differentially
437 expressed in *Flt3*$^{ITD/+}$*; Runx1*$^{\Delta/+}$ HPCs and those that Shih et al. found to be
438 differentially expressed in *Flt3*^{ITD}*; Tet2*$^{\Delta/\Delta}$ HPCs (Shih et al., 2015) (Fig. 9B). This
439 suggests that FLT3^{ITD} can cooperate with diverse mutations to induce a
440 conserved set of target genes.
441 We used hierarchical clustering to better visualize differences in gene
442 expression at P0 and P14. This approach did show some differences between
443 wild type and *Flt3*$^{ITD/+}$*; Runx1*$^{\Delta/+}$ HPCs at P0 (Fig. 9C), but much greater
444 differences were observed at P14 for most target genes (Fig. 9C, D). Of the 25
445 most differentially expressed genes in P14 *Flt3*$^{ITD/+}$*; Runx1*$^{\Delta/+}$ HPCs, only three –
446 *Nov*, *Bhlhe40* and *Mboat2* – were induced equally at both P0 and P14 (Figs. 9D,
447 Fig. 9 – source data table 1). The remaining genes showed only a partial change
448 in expression at P0 (e.g. *Socs2*) or no change in expression (e.g. *Adgre1*, *Dusp6*,
449 *Gem*, *Postn*) (Fig. 9D). GSEA also showed differences in the transcriptional
450 programs of P0 and P14 *Flt3*$^{ITD/+}$*; Runx1*$^{\Delta/+}$ HPCs. Several Gene Ontology and
451 Oncogenic Signatures gene sets were enriched in P14 *Flt3*$^{ITD/+}$*; Runx1*$^{\Delta/+}$ HPCs
452 relative to wild type controls, the most significant of which included genes that
453 are negatively regulated by mTOR (Majumder et al., 2004), genes that inhibit
454 apoptosis (Gene Ontology) and c-myc targets (Bild et al., 2006) (Fig. 9E). These
455 gene sets were not significantly enriched in P0 HSCs with the exception of the
456 anti-apoptotic gene set, which was paradoxically enriched in wild type HPCs

457 relative to *Flt3*$^{ITD/+}$*; Runx1*$^{\Delta/+}$ (Fig. 9E). Altogether, the data show that cooperating
458 *Flt3*^{ITD} and *Runx1* mutations – and likely other cooperating mutations – have
459 developmental context-specific effects on gene expression.
460
461 **Discussion**
462 Our data offer a potential explanation for why *FLT3*^{ITD} mutations are rare
463 in infants and young children with AML. The mutant FLT3^{ITD} protein hyper-
464 activates STAT5 in hematopoietic progenitors during both fetal and adult stages
465 of development, yet its effects on transcription are realized selectively in adult
466 progenitors. Even cooperative interactions between *Flt3*^{ITD} and *Runx1*
467 heterozygous mutations are blunted during fetal and perinatal stages. Thus,
468 *FLT3*^{ITD} mutations may occur disproportionately in older children and adults with
469 AML because they are less able to activate key effectors of leukemogenesis
470 during earlier stages of life.
471
472 *Flt3*^{ITD} *has distinct STAT5-dependent and STAT5-independent effects on self-*
473 *renewal and myeloid commitment, respectively*
474 In the course of these studies, we discovered that *Stat5a/b* deletion
475 exacerbates, rather than rescues, the HSC depletion, HPC/GMP expansion and
476 MPN phenotypes of *Flt3*$^{ITD/+}$ mice. Furthermore, FLT3^{ITD} ectopically activated
477 STAT5-dependent self-renewal programs in HPCs (Fig. 7). These unanticipated
478 findings suggest that FLT3^{ITD} activates both STAT5-dependent and STAT5-
479 independent signal transduction pathways and that these pathways have

opposing effects on self-renewal and myeloid commitment. In this model, STAT5-independent myeloid commitment programs outweigh STAT5-dependent self-renewal programs in *Flt3*^{ITD} mutant bone marrow so the HSC pool becomes depleted (Fig. 6I and Fig. 7). *Stat5a/b* deletion can shift the balance further in favor of differentiation, though cooperating mutations may ultimately allow STAT5-dependent self-renewal programs to predominate in transformed AML cells.

The STAT5-independent pathways that antagonize HSC self-renewal and promote myeloid progenitor expansion remain unclear. While the MAPK pathway was hyper-activated in postnatal *Flt3*$^{ITD/+}$ HSCs and HPCs, MEK inhibition did not prevent, or even reduce, HSC depletion or HPC expansion in these mice (Fig. 5). Other candidate pathways, including STAT3 and PI3K, were not activated by FLT3^{ITD} (Fig. 4A). It is possible that low levels of signal transduction via these pathways were undetectable by Western blot but nevertheless functionally important. It is also possible that an un-interrogated pathway, such as NF-κB or CDK1 (Gerloff et al., 2015; Radomska et al., 2012), could promote myeloid commitment and antagonize STAT5. Our GSEA data did show increased expression of inflammatory cytokine receptors in *Stat5a/b*-deficient, *Flt3*^{ITD} HPCs. This raises the intriguing possibility that inflammatory cytokines could promote differentiation of *Flt3*^{ITD} mutant progenitors, and perhaps AML cells. Additional genetic studies are needed to resolve whether these transcriptional changes are a cause or a consequence of enhanced lineage commitment in *Flt3*^{ITD} mutant HPCs..

Developmental programming, re-programming and the origins of pediatric and adult malignancies

Heterochronic genes have been implicated in cancer pathogenesis (Shyh-Chang and Daley, 2013). For example, hepatoblastomas, Wilm's tumors and most neuroblastomas present early in life, and they often express the oncofetal proteins LIN28 or LIN28B at high levels to help maintain the primitive differentiation states of their respective anlagen (Diskin et al., 2012; Molenaar et al., 2012; Nguyen et al., 2014; Urbach et al., 2014). Adult hepatocellular carcinomas, germ cell tumors and ovarian carcinomas often ectopically activate LIN28 or LIN28B to restore oncofetal programs (Viswanathan et al., 2009). MLL-rearranged leukemias have similarly been shown to express embryonic stem cell-related genes (Somervaille et al., 2009), and $BRAF^{V600E}$ driven melanoma was recently shown to arise from melanocytes that first de-differentiate into primitive neural crest progenitors (Kaufman et al., 2016). In each of these cases, it is easy to appreciate why maintaining or restoring a primitive cell identity might accelerate transformation – fetal cells can proliferate rapidly without differentiating or senescing. However, it is then curious as to why pediatric malignancies are relatively uncommon. Does this simply reflect greater fidelity of the genome at early ages, or are other factors at work?

Our data suggest that the transcriptional regulatory programs of fetal progenitors may, in fact, be protective against some mechanisms of transformation. Fetal and adult progenitors interpret $FLT3^{ITD}$-derived signals

differently, as evidenced by their distinct transcriptional responses (Figs. 7 and 8), and this constrains the ability of $FLT3^{ITD}$ to transform fetal progenitors. Either they lack key transcriptional co-activators, or the epigenetic landscape of fetal progenitors suppresses $FLT3^{ITD}$ target gene activation. Further work is needed to understand the cis- and trans-regulatory elements that determine when and how individual mutations are competent to transform. If we can understand how normal developmental programs interact with genetic mutations to cause malignancies, it may be possible to target these interactions therapeutically.

Materials and methods

Mouse strains

The *Flt3*^{ITD} RRID:IMSR_JAX:011112 (Lee et al., 2007), *Runx1*^{f} RRID:IMSR_JAX:008772 (Taniuchi et al., 2002), *Stat5a/b*^{f} RRID:MMRRC_032053-JAX (Cui et al., 2004), *Rictor*^{f} RRID:IMSR_JAX:020649 (Magee et al., 2012), *Vav1-Cre* RRID:IMSR_JAX:008610 (Siegemund et al., 2015) and *Mx1-Cre* RRID:IMSR_JAX:003556 (Kuhn et al., 1995) mouse strains have all been previously described and were obtained from The Jackson Laboratory. These lines were all on a pure C57BL/6 background. Expression of *Mx1-Cre* was induced by three intraperitoneal injections of pIpC (GE Life Sciences; 10 μg/dose) over five days beginning 6 weeks after birth. PD0325901 (Cayman Chemicals) was suspended in 0.5% hydroxypropylmethylcellulose vehicle (Sigma) and administered by oral gavage as described in the text. All mice were housed in the Department for Comparative Medicine at Washington

University. All animal procedures were approved by the Washington University Committees on the Use and Care of Animals.

Isolation of HSCs and flow cytometry

Bone marrow cells were obtained by flushing the long bones (tibias and femurs) or by crushing long bones, pelvic bones and vertebrae with a mortar and pestle in calcium and magnesium-free Hank's buffered salt solution (HBSS), supplemented with 2% heat inactivated bovine serum (Gibco). Splenocytes were obtained by macerating spleens with frosted slides. Single cell suspensions were filtered through a 40 um cell strainer (Fisher). The cells were then stained for 20 minutes with fluorescently conjugated antibodies, washed with HBSS + 2% bovine serum and resuspended for analysis. Cell counts were measured by hemocytometer. The following antibodies were used for flow cytometry, all were from Biolegend except as indicated: CD150 (TC15-12F12.2), CD48 (HM48-1), Sca1 (D7), c-Kit (2B8), Ter119 (Ter-119), CD3 (17A2), CD11b (M1/70), Gr-1 (RB6-8C5), B220 (RA3-6B2), CD8a (53-6.7), CD34 (eBioscience, RAM34), CD2 (RM2-5), CD45.1 (A20), CD45.2 (104), CD127 (A7R340), CD16/32 (93) and FLT3/CD135 (A2F10). Lineage stains for all experiments included CD2, CD3, CD8a, Ter119, B220 and Gr1. Antibodies to CD4 and CD11b were omitted from the lineage stains because they are expressed on fetal HSCs at low levels. Unless otherwise indicated, we used the following surface marker phenotypes to define cell populations: HSCs ($CD150^+$, $CD48^-Lineage^-$, $Sca1^+$, $c\text{-}kit^+$), HPCs ($CD48^-Lineage^-$, $Sca1^+$, $c\text{-}kit^+$), and GMPs ($Lineage^-$, $Sca1^-$, $CD127^-$, $c\text{-}kit^+$,

572 CD34^{+}, CD16/32^{+}). Non-viable cells were excluded from analyses by 4',6-
573 diamidino-2-phenylindone (DAPI) staining (1 μg/ml). When HSCs and HPCs
574 were isolated for Western blotting or RNA collection, c-kit^{+} cells were enriched
575 prior to sorting by selection with paramagnetic beads (Miltenyi Biotec). Flow
576 cytometry was performed on a BD FACSAria Fusion flow cytometer (BD
577 Biosciences).
578
579 *Limiting dilution long-term repopulation assays*
580 Eight to ten week old C57BL/6Ka-Thy-1.2 (CD45.1) recipient mice were
581 given two doses of 550 rad delivered at least 3 hours apart. Donor fetal liver or
582 bone marrow cells were mixed with competitor bone marrow cells at the doses
583 indicated in the text and injected via the retroorbital sinus. To assess donor
584 chimerism, peripheral blood was obtained from the submandibular veins of
585 recipient mice at the indicated times after transplantation. Blood was subjected to
586 ammonium-chloride lysis of the red blood cells and leukocytes were stained with
587 antibodies to CD45.2, CD45.1, B220, CD3, CD11b and Gr-1 to assess
588 multilineage engraftment. Functional HSC frequencies were calculated and
589 compared by using Extreme Limiting Dilution Analysis (Hu and Smyth, 2009). For
590 secondary transplants, mice were injected with 3 million cells from the bone
591 marrow of primary recipient mice.
592
593
594 *Quantitative RT-PCR*
595 RNA was isolated from HSCs with RNAeasy micro plus columns (Qiagen)
596 and converted to cDNA with Superscript III reverse transcriptase (Lifetech).

Quantitative RT-PCR assays were performed with Taqman Gene Expression Assays specific to mouse *Flt3* and β-actin (Lifetech). Analysis was performed with a Mx3005P qPCR system (Agilent). Samples were normalized based on β-actin expression.

Western blots

Twenty-five thousand HSC/MPPs, HPCs or GMPs were double sorted into Trichloracetic acid (TCA), and the volume was adjusted to a final concentration of 10% TCA. Extracts were incubated for 15 minutes on ice and centrifuged at 16,100xg at 4°C for 10 minutes. Precipitates were washed in acetone twice and dried. The pellets were solubilized in 9M urea, 2% Triton X-100, 1% DTT. LDS loading buffer (Lifetech) was added and the pellet was heated at 70°C for 10 minutes. Samples were separated on Bis-Tris polyacrylamide gels (Lifetech) and transferred to PVDF membrane (Lifetech). All antibodies were from Cell Signaling Technologies except as indicated: P-STAT5 (4322), Total STAT5 (9363), P-STAT3 (9145), Total STAT3 (9139), P-ERK1/2 (4370), Total ERK1/2 (4696), P-AKT Ser473 (4060), P-AKT T308 (13038), Total AKT (4691), α-TUBULIN (3873), β-ACTIN (Santa Cruz Bioscience, clone AC-17), HRP-anti-Rabbit IgG (7074) and HRP-anti-mouse IgG (7076). Blots were developed with the SuperSignal West Femto or Pico chemiluminescence kits (Thermo Scientific). Blots were stripped (1% SDS, 25 mM glycine pH 2) prior to re-probing.

Cytospins

Bone marrow cells were isolated and spun onto glass slides using a Shandon Cytospin 3. The slides were stained using Protocol Hema 3 Wright-Giemsa stain (Fisher Scientific). All slides were reviewed by a pediatric hematologist (JAM or ASC).

Statistical analysis

In all cases, multiple independent experiments were performed on at least three different days to verify that the data are reproducible. Grouped data reflect biological replicates (i.e. independent mice) and are represented by mean +/- standard deviation. Statistical comparisons between groups were made with the two-tailed Student's t-test except as noted in the figure legends. When multiple genotypes were compared, statistical significance was determined by performing a one-way ANOVA followed by a Holm-Sidak post-hoc test to correct for multiple comparisons. For transplantation experiments, the percentages of mice with multilineage reconstitution were compared with the Fisher's exact test. All comparisons were performed with GraphPad Prism 6, RRID:SCR_002798.

Gene expression analysis

Ten thousand HSCs or HPCs were double sorted directly into RLT plus RNA lysis buffer (Qiagen) and RNA was isolated with RNAeasy micro plus columns (Qiagen). Transcripts were amplified with the WTA2 kit (Sigma) with the Kreatech ULS RNA labeling kit (Kreatech Diagnostics). Labeled cDNA was hybridized to Agilent Mouse 8x60K microarrays and analyzed with an Agilent C-

643 class scanner. Signal data were assembled and processed in Partek
644 RRID:SCR_011860, and samples were compared by Linear Models for
645 Microarrays, RRID:SCR_010943 (Ritchie et al., 2015; Smyth, 2004). Adjusted p-
646 values were calculated by the Benjamini and Hochberg false discovery rate
647 (Benjamini and Hochberg, 1995). Z-scores were calculated as previously
648 described (Cheadle et al., 2003). Hierarchical cluster analysis was performed
649 with Cluster 3.0 and visualized with Java TreeView; RRID:SCR_013505 and
650 RRID:SCR_013503 (Eisen et al., 1998). Principal component analyses and
651 Euclidean distance comparisons (by permutation testing) were performed with
652 the R software environment. Microarray data sets have been deposited into
653 Gene Expression Omnibus (GSE81153). GSEA was performed using gene sets
654 that were generated as cited in the text, or with gene sets curated in the MSigDB
655 databases; RRID:SCR_003199 (Subramanian et al., 2005).
656

657 **Acknowledgements**

658 This work was supported by grants from the Department of Defense
659 (CA130124), the St. Baldrick's Foundation, Hyundai Hope on Wheels, the
660 Gabrielle's Angel Foundation for Cancer Research and the Children's Discovery
661 Institute of Washington University and St. Louis Children's Hospital. JAM is a
662 scholar of the Child Health Research Center for Excellence in Developmental
663 Biology at Washington University (K12-HD076224). ASC is supported by a
664 training grant to the Washington University Department of Pediatrics
665 (5T32HD043010-12). We thank Jenna Voigtmann for technical assistance. We

666 thank D. Bhattacharya, G. Challen, I. Maillard and R. Signer for comments on the
667 manuscript.
668
669

References

Andersson, A.K., Ma, J., Wang, J., Chen, X., Gedman, A.L., Dang, J., Nakitandwe, J., Holmfeldt, L., Parker, M., Easton, J.*, et al.* (2015). The landscape of somatic mutations in infant MLL-rearranged acute lymphoblastic leukemias. Nat Genet *47*, 330-337.

Baldridge, M.T., King, K.Y., Boles, N.C., Weksberg, D.C., and Goodell, M.A. (2010). Quiescent haematopoietic stem cells are activated by IFN-gamma in response to chronic infection. Nature *465*, 793-797.

Benjamini, Y., and Hochberg, Y. (1995). Controlling the False Discovery Rate - a Practical and Powerful Approach to Multiple Testing. J Roy Stat Soc B Met *57*, 289-300.

Benz, C., Copley, M.R., Kent, D.G., Wohrer, S., Cortes, A., Aghaeepour, N., Ma, E., Mader, H., Rowe, K., Day, C.*, et al.* (2012). Hematopoietic stem cell subtypes expand differentially during development and display distinct lymphopoietic programs. Cell Stem Cell *10*, 273-283.

Bild, A.H., Yao, G., Chang, J.T., Wang, Q., Potti, A., Chasse, D., Joshi, M.B., Harpole, D., Lancaster, J.M., Berchuck, A.*, et al.* (2006). Oncogenic pathway signatures in human cancers as a guide to targeted therapies. Nature *439*, 353-357.

689 Bowie, M.B., McKnight, K.D., Kent, D.G., McCaffrey, L., Hoodless, P.A., and
690 Eaves, C.J. (2006). Hematopoietic stem cells proliferate until after birth and show
691 a reversible phase-specific engraftment defect. J Clin Invest *116*, 2808-2816.

692 Buza-Vidas, N., Woll, P., Hultquist, A., Duarte, S., Lutteropp, M., Bouriez-Jones,
693 T., Ferry, H., Luc, S., and Jacobsen, S.E. (2011). FLT3 expression initiates in
694 fully multipotent mouse hematopoietic progenitor cells. Blood *118*, 1544-1548.

695 Cai, X., Gaudet, J.J., Mangan, J.K., Chen, M.J., De Obaldia, M.E., Oo, Z., Ernst,
696 P., and Speck, N.A. (2011). Runx1 loss minimally impacts long-term
697 hematopoietic stem cells. PLoS One *6*, e28430.

698 Cancer Genome Atlas Research Network (2013). Genomic and epigenomic
699 landscapes of adult de novo acute myeloid leukemia. N Engl J Med *368*, 2059-
700 2074.

701 Chaudhury, S.S., Morison, J.K., Gibson, B.E., and Keeshan, K. (2015). Insights
702 into cell ontogeny, age, and acute myeloid leukemia. Exp Hematol *43*, 745-755.

703 Cheadle, C., Vawter, M.P., Freed, W.J., and Becker, K.G. (2003). Analysis of
704 microarray data using Z score transformation. J Mol Diagn *5*, 73-81.

705 Choudhary, C., Brandts, C., Schwable, J., Tickenbrock, L., Sargin, B., Ueker, A.,
706 Bohmer, F.D., Berdel, W.E., Muller-Tidow, C., and Serve, H. (2007). Activation
707 mechanisms of STAT5 by oncogenic Flt3-ITD. Blood *110*, 370-374.

708 Chu, S.H., Heiser, D., Li, L., Kaplan, I., Collector, M., Huso, D., Sharkis, S.J.,
709 Civin, C., and Small, D. (2012). FLT3-ITD knockin impairs hematopoietic stem
710 cell quiescence/homeostasis, leading to myeloproliferative neoplasm. Cell Stem
711 Cell *11*, 346-358.

712 Copley, M.R., Babovic, S., Benz, C., Knapp, D.J., Beer, P.A., Kent, D.G.,
713 Wohrer, S., Treloar, D.Q., Day, C., Rowe, K.*, et al.* (2013). The Lin28b-let-7-
714 Hmga2 axis determines the higher self-renewal potential of fetal haematopoietic
715 stem cells. Nat Cell Biol *15*, 916-925.

716 Cui, Y., Riedlinger, G., Miyoshi, K., Tang, W., Li, C., Deng, C.X., Robinson, G.W.,
717 and Hennighausen, L. (2004). Inactivation of Stat5 in mouse mammary
718 epithelium during pregnancy reveals distinct functions in cell proliferation,
719 survival, and differentiation. Mol Cell Biol *24*, 8037-8047.

720 Diskin, S.J., Capasso, M., Schnepp, R.W., Cole, K.A., Attiyeh, E.F., Hou, C.,
721 Diamond, M., Carpenter, E.L., Winter, C., Lee, H.*, et al.* (2012). Common
722 variation at 6q16 within HACE1 and LIN28B influences susceptibility to
723 neuroblastoma. Nat Genet *44*, 1126-1130.

724 Downing, J.R., and Shannon, K.M. (2002). Acute leukemia: a pediatric
725 perspective. Cancer Cell *2*, 437-445.

726 Eisen, M.B., Spellman, P.T., Brown, P.O., and Botstein, D. (1998). Cluster
727 analysis and display of genome-wide expression patterns. Proc Natl Acad Sci U
728 S A *95*, 14863-14868.

729 Essers, M.A., Offner, S., Blanco-Bose, W.E., Waibler, Z., Kalinke, U., Duchosal,
730 M.A., and Trumpp, A. (2009). IFNalpha activates dormant haematopoietic stem
731 cells in vivo. Nature *458*, 904-908.

732 Foudi, A., Hochedlinger, K., Van Buren, D., Schindler, J.W., Jaenisch, R., Carey,
733 V., and Hock, H. (2009). Analysis of histone 2B-GFP retention reveals slowly
734 cycling hematopoietic stem cells. Nat Biotechnol *27*, 84-90.

735 Gerloff, D., Grundler, R., Wurm, A.A., Brauer-Hartmann, D., Katzerke, C.,
736 Hartmann, J.U., Madan, V., Muller-Tidow, C., Duyster, J., Tenen, D.G.*, et al.*
737 (2015). NF-kappaB/STAT5/miR-155 network targets PU.1 in FLT3-ITD-driven
738 acute myeloid leukemia. Leukemia *29*, 535-547.

739 He, S., Nakada, D., and Morrison, S.J. (2009). Mechanisms of stem cell self-
740 renewal. Annu Rev Cell Dev Biol *25*, 377-406.

741 Ho, P.A., Kutny, M.A., Alonzo, T.A., Gerbing, R.B., Joaquin, J., Raimondi, S.C.,
742 Gamis, A.S., and Meshinchi, S. (2011). Leukemic mutations in the methylation-
743 associated genes DNMT3A and IDH2 are rare events in pediatric AML: a report
744 from the Children's Oncology Group. Pediatric blood & cancer *57*, 204-209.

745 Hock, H., Meade, E., Medeiros, S., Schindler, J.W., Valk, P.J., Fujiwara, Y., and
746 Orkin, S.H. (2004). Tel/Etv6 is an essential and selective regulator of adult
747 hematopoietic stem cell survival. Genes Dev *18*, 2336-2341.

748 Horton, S.J., Jaques, J., Woolthuis, C., van Dijk, J., Mesuraca, M., Huls, G.,
749 Morrone, G., Vellenga, E., and Schuringa, J.J. (2013). MLL-AF9-mediated
750 immortalization of human hematopoietic cells along different lineages changes
751 during ontogeny. Leukemia *27*, 1116-1126.

752 Hu, Y., and Smyth, G.K. (2009). ELDA: extreme limiting dilution analysis for
753 comparing depleted and enriched populations in stem cell and other assays. J
754 Immunol Methods *347*, 70-78.

755 Huang, J., Liu, X., Li, D., Shao, Z., Cao, H., Zhang, Y., Trompouki, E., Bowman,
756 T.V., Zon, L.I., Yuan, G.C.*, et al.* (2016). Dynamic Control of Enhancer
757 Repertoires Drives Lineage and Stage-Specific Transcription during
758 Hematopoiesis. Dev Cell *36*, 9-23.

759 Ivanova, N.B., Dimos, J.T., Schaniel, C., Hackney, J.A., Moore, K.A., and
760 Lemischka, I.R. (2002). A stem cell molecular signature. Science *298*, 601-604.

761 Jan, M., Snyder, T.M., Corces-Zimmerman, M.R., Vyas, P., Weissman, I.L.,
762 Quake, S.R., and Majeti, R. (2012). Clonal evolution of preleukemic
763 hematopoietic stem cells precedes human acute myeloid leukemia. Sci Transl
764 Med *4*, 149ra118.

765 Jones, M., Chase, J., Brinkmeier, M., Xu, J., Weinberg, D.N., Schira, J.,
766 Friedman, A., Malek, S., Grembecka, J., Cierpicki, T.*, et al.* (2015). Ash1l
767 controls quiescence and self-renewal potential in hematopoietic stem cells. J Clin
768 Invest *125*, 2007-2020.

769 Jude, C.D., Climer, L., Xu, D., Artinger, E., Fisher, J.K., and Ernst, P. (2007).
770 Unique and independent roles for MLL in adult hematopoietic stem cells and
771 progenitors. Cell Stem Cell *1*, 324-337.

772 Kaufman, C.K., Mosimann, C., Fan, Z.P., Yang, S., Thomas, A.J., Ablain, J., Tan,
773 J.L., Fogley, R.D., van Rooijen, E., Hagedorn, E.J.*, et al.* (2016). A zebrafish
774 melanoma model reveals emergence of neural crest identity during melanoma
775 initiation. Science *351*, aad2197.

776 Kim, I., Saunders, T.L., and Morrison, S.J. (2007). Sox17 dependence
777 distinguishes the transcriptional regulation of fetal from adult hematopoietic stem
778 cells. Cell *130*, 470-483.

779 Kuhn, R., Schwenk, F., Aguet, M., and Rajewsky, K. (1995). Inducible gene
780 targeting in mice. Science *269*, 1427-1429.

781 Lee, B.H., Tothova, Z., Levine, R.L., Anderson, K., Buza-Vidas, N., Cullen, D.E.,
782 McDowell, E.P., Adelsperger, J., Frohling, S., Huntly, B.J.*, et al.* (2007). FLT3
783 mutations confer enhanced proliferation and survival properties to multipotent

progenitors in a murine model of chronic myelomonocytic leukemia. Cancer Cell *12*, 367-380.

Li, L., Piloto, O., Nguyen, H.B., Greenberg, K., Takamiya, K., Racke, F., Huso, D., and Small, D. (2008). Knock-in of an internal tandem duplication mutation into murine FLT3 confers myeloproliferative disease in a mouse model. Blood *111*, 3849-3858.

Liang, D.C., Liu, H.C., Yang, C.P., Jaing, T.H., Hung, I.J., Yeh, T.C., Chen, S.H., Hou, J.Y., Huang, Y.J., Shih, Y.S.*, et al.* (2013). Cooperating gene mutations in childhood acute myeloid leukemia with special reference on mutations of ASXL1, TET2, IDH1, IDH2, and DNMT3A. Blood *121*, 2988-2995.

Magee, J.A., Ikenoue, T., Nakada, D., Lee, J.Y., Guan, K.L., and Morrison, S.J. (2012). Temporal changes in PTEN and mTORC2 regulation of hematopoietic stem cell self-renewal and leukemia suppression. Cell Stem Cell *11*, 415-428.

Majumder, P.K., Febbo, P.G., Bikoff, R., Berger, R., Xue, Q., McMahon, L.M., Manola, J., Brugarolas, J., McDonnell, T.J., Golub, T.R.*, et al.* (2004). mTOR inhibition reverses Akt-dependent prostate intraepithelial neoplasia through regulation of apoptotic and HIF-1-dependent pathways. Nat Med *10*, 594-601.

Mead, A.J., Kharazi, S., Atkinson, D., Macaulay, I., Pecquet, C., Loughran, S., Lutteropp, M., Woll, P., Chowdhury, O., Luc, S.*, et al.* (2013). FLT3-ITDs instruct

803 a myeloid differentiation and transformation bias in lymphomyeloid multipotent
804 progenitors. Cell reports *3*, 1766-1776.

805 Meshinchi, S., Alonzo, T.A., Stirewalt, D.L., Zwaan, M., Zimmerman, M.,
806 Reinhardt, D., Kaspers, G.J., Heerema, N.A., Gerbing, R., Lange, B.J.*, et al.*
807 (2006). Clinical implications of FLT3 mutations in pediatric AML. Blood *108*,
808 3654-3661.

809 Molenaar, J.J., Domingo-Fernandez, R., Ebus, M.E., Lindner, S., Koster, J.,
810 Drabek, K., Mestdagh, P., van Sluis, P., Valentijn, L.J., van Nes, J.*, et al.* (2012).
811 LIN28B induces neuroblastoma and enhances MYCN levels via let-7
812 suppression. Nat Genet *44*, 1199-1206.

813 Mupo, A., Celani, L., Dovey, O., Cooper, J.L., Grove, C., Rad, R., Sportoletti, P.,
814 Falini, B., Bradley, A., and Vassiliou, G.S. (2013). A powerful molecular synergy
815 between mutant Nucleophosmin and Flt3-ITD drives acute myeloid leukemia in
816 mice. Leukemia *27*, 1917-1920.

817 Nguyen, L.H., Robinton, D.A., Seligson, M.T., Wu, L., Li, L., Rakheja, D.,
818 Comerford, S.A., Ramezani, S., Sun, X., Parikh, M.S.*, et al.* (2014). Lin28b is
819 sufficient to drive liver cancer and necessary for its maintenance in murine
820 models. Cancer Cell *26*, 248-261.

821 Pietras, E.M., Mirantes-Barbeito, C., Fong, S., Loeffler, D., Kovtonyuk, L.V.,
822 Zhang, S., Lakshminarasimhan, R., Chin, C.P., Techner, J.M., Will, B.*, et al.*

(2016). Chronic interleukin-1 exposure drives haematopoietic stem cells towards precocious myeloid differentiation at the expense of self-renewal. Nat Cell Biol *18*, 607-618.

Pietras, E.M., and Passegue, E. (2013). Linking HSCs to their youth. Nat Cell Biol *15*, 885-887.

Pine, S.R., Guo, Q., Yin, C., Jayabose, S., Druschel, C.M., and Sandoval, C. (2007). Incidence and clinical implications of GATA1 mutations in newborns with Down syndrome. Blood *110*, 2128-2131.

Porter, S.N., Cluster, A.S., Signer, R.A., Voigtmann, J., Monlish, D.A., Schuettpelz, L.G., and Magee, J.A. (2016). Pten Cell Autonomously Modulates the Hematopoietic Stem Cell Response to Inflammatory Cytokines. Stem Cell Reports *6*, 806-814.

Radomska, H.S., Alberich-Jorda, M., Will, B., Gonzalez, D., Delwel, R., and Tenen, D.G. (2012). Targeting CDK1 promotes FLT3-activated acute myeloid leukemia differentiation through C/EBPalpha. J Clin Invest *122*, 2955-2966.

Radomska, H.S., Basseres, D.S., Zheng, R., Zhang, P., Dayaram, T., Yamamoto, Y., Sternberg, D.W., Lokker, N., Giese, N.A., Bohlander, S.K.*, et al.* (2006). Block of C/EBP alpha function by phosphorylation in acute myeloid leukemia with FLT3 activating mutations. J Exp Med *203*, 371-381.

842 Rau, R., Magoon, D., Greenblatt, S., Li, L., Annesley, C., Duffield, A.S., Huso, D.,
843 McIntyre, E., Clohessy, J.G., Reschke, M.*, et al.* (2014). NPMc+ cooperates with
844 Flt3/ITD mutations to cause acute leukemia recapitulating human disease. Exp
845 Hematol *42*, 101-113 e105.

846 Ritchie, M.E., Phipson, B., Wu, D., Hu, Y., Law, C.W., Shi, W., and Smyth, G.K.
847 (2015). limma powers differential expression analyses for RNA-sequencing and
848 microarray studies. Nucleic Acids Res *43*, e47.

849 Schnittger, S., Dicker, F., Kern, W., Wendland, N., Sundermann, J., Alpermann,
850 T., Haferlach, C., and Haferlach, T. (2011). RUNX1 mutations are frequent in de
851 novo AML with noncomplex karyotype and confer an unfavorable prognosis.
852 Blood *117*, 2348-2357.

853 Shih, A.H., Jiang, Y., Meydan, C., Shank, K., Pandey, S., Barreyro, L., Antony-
854 Debre, I., Viale, A., Socci, N., Sun, Y.*, et al.* (2015). Mutational cooperativity
855 linked to combinatorial epigenetic gain of function in acute myeloid leukemia.
856 Cancer Cell *27*, 502-515.

857 Shyh-Chang, N., and Daley, G.Q. (2013). Lin28: primal regulator of growth and
858 metabolism in stem cells. Cell Stem Cell *12*, 395-406.

859 Siegemund, S., Shepherd, J., Xiao, C., and Sauer, K. (2015). hCD2-iCre and
860 Vav-iCre mediated gene recombination patterns in murine hematopoietic cells.
861 PLoS One *10*, e0124661.

862 Smyth, G.K. (2004). Linear models and empirical bayes methods for assessing
863 differential expression in microarray experiments. Statistical applications in
864 genetics and molecular biology *3*, Article3.

865 Somervaille, T.C., Matheny, C.J., Spencer, G.J., Iwasaki, M., Rinn, J.L., Witten,
866 D.M., Chang, H.Y., Shurtleff, S.A., Downing, J.R., and Cleary, M.L. (2009).
867 Hierarchical maintenance of MLL myeloid leukemia stem cells employs a
868 transcriptional program shared with embryonic rather than adult stem cells. Cell
869 Stem Cell *4*, 129-140.

870 Subramanian, A., Tamayo, P., Mootha, V.K., Mukherjee, S., Ebert, B.L., Gillette,
871 M.A., Paulovich, A., Pomeroy, S.L., Golub, T.R., Lander, E.S.*, et al.* (2005).
872 Gene set enrichment analysis: a knowledge-based approach for interpreting
873 genome-wide expression profiles. Proc Natl Acad Sci U S A *102*, 15545-15550.

874 Taniuchi, I., Osato, M., Egawa, T., Sunshine, M.J., Bae, S.C., Komori, T., Ito, Y.,
875 and Littman, D.R. (2002). Differential requirements for Runx proteins in CD4
876 repression and epigenetic silencing during T lymphocyte development. Cell *111*,
877 621-633.

878 Urbach, A., Yermalovich, A., Zhang, J., Spina, C.S., Zhu, H., Perez-Atayde, A.R.,
879 Shukrun, R., Charlton, J., Sebire, N., Mifsud, W.*, et al.* (2014). Lin28 sustains
880 early renal progenitors and induces Wilms tumor. Genes Dev *28*, 971-982.

881 Viswanathan, S.R., Powers, J.T., Einhorn, W., Hoshida, Y., Ng, T.L., Toffanin, S.,
882 O'Sullivan, M., Lu, J., Phillips, L.A., Lockhart, V.L.*, et al.* (2009). Lin28 promotes
883 transformation and is associated with advanced human malignancies. Nat Genet
884 *41*, 843-848.

885 Wang, Y., Kim, E., Wang, X., Novitch, B.G., Yoshikawa, K., Chang, L.S., and
886 Zhu, Y. (2012). ERK inhibition rescues defects in fate specification of Nf1-
887 deficient neural progenitors and brain abnormalities. Cell *150*, 816-830.

888 Wang, Z., Li, G., Tse, W., and Bunting, K.D. (2009). Conditional deletion of
889 STAT5 in adult mouse hematopoietic stem cells causes loss of quiescence and
890 permits efficient nonablative stem cell replacement. Blood *113*, 4856-4865.

891 Welch, J.S., Ley, T.J., Link, D.C., Miller, C.A., Larson, D.E., Koboldt, D.C.,
892 Wartman, L.D., Lamprecht, T.L., Liu, F., Xia, J.*, et al.* (2012). The origin and
893 evolution of mutations in acute myeloid leukemia. Cell *150*, 264-278.

894 Wilson, A., Laurenti, E., Oser, G., van der Wath, R.C., Blanco-Bose, W.,
895 Jaworski, M., Offner, S., Dunant, C.F., Eshkind, L., Bockamp, E.*, et al.* (2008).
896 Hematopoietic stem cells reversibly switch from dormancy to self-renewal during
897 homeostasis and repair. Cell *135*, 1118-1129.

898 Xu, J., Shao, Z., Glass, K., Bauer, D.E., Pinello, L., Van Handel, B., Hou, S.,
899 Stamatoyannopoulos, J.A., Mikkola, H.K., Yuan, G.C.*, et al.* (2012).

900 Combinatorial assembly of developmental stage-specific enhancers controls
901 gene expression programs during human erythropoiesis. Dev Cell *23*, 796-811.

902 Yuan, J., Nguyen, C.K., Liu, X., Kanellopoulou, C., and Muljo, S.A. (2012).
903 Lin28b reprograms adult bone marrow hematopoietic progenitors to mediate
904 fetal-like lymphopoiesis. Science *335*, 1195-1200.

905 Zhu, B.M., McLaughlin, S.K., Na, R., Liu, J., Cui, Y., Martin, C., Kimura, A.,
906 Robinson, G.W., Andrews, N.C., and Hennighausen, L. (2008). Hematopoietic-
907 specific Stat5-null mice display microcytic hypochromic anemia associated with
908 reduced transferrin receptor gene expression. Blood *112*, 2071-2080.

909 Zwaan, C.M., Meshinchi, S., Radich, J.P., Veerman, A.J., Huismans, D.R.,
910 Munske, L., Podleschny, M., Hahlen, K., Pieters, R., Zimmermann, M.*, et al.*
911 (2003). FLT3 internal tandem duplication in 234 children with acute myeloid
912 leukemia: prognostic significance and relation to cellular drug resistance. Blood
913 *102*, 2387-2394.
914
915

Figure Legends

Figure 1. *Flt3*^{ITD} causes HSC depletion in adult but not fetal mice.

(A) *Flt3* transcript expression in fetal and adult HSCs and HPCs relative to fetal HSCs; n=4-9. (B) FLT3 expression in fetal and adult HSC/HPCs (Lineage$^-$ Sca1$^+$c-kit$^+$) and unfractionated fetal liver or bone marrow cells, as determined by flow cytometry (N=3). (C) HSC numbers in two tibias and femurs from adult wild type and *Flt3*^{ITD} mice; n=12-16. (D) HSC numbers in fetal livers from E14.5 wild type and *Flt3*^{ITD} mice; n=9-20. (E) Spleen HSC frequency in adult wild type and *Flt3*$^{ITD/ITD}$ mice; n=4-5. (F, G) Limiting dilution analyses using adult bone marrow (F) or E14.5 fetal liver cells (G); n=9-10 recipients per cell dose. Wild type and *Flt3*$^{ITD/ITD}$ HSC frequencies were calculated by extreme limiting dilution analysis. (H, I) Frequencies of donor (CD45.2) and competitor (CD45.1) HSCs (H) and donor bone marrow cells (I) in primary recipients of 100,000 fetal liver cells; n=15 per genotype. (J) Frequencies of CD45.2+ peripheral blood cells in secondary recipients of donor cells that originated from wild type or *Flt3*$^{ITD/ITD}$ fetal livers; n=12-14. (K) Percentage of secondary recipient mice with multilineage donor reconstitution. In all panels, error bars indicate standard deviations and n reflects biological replicates. * $p<0.05$, *** $p<0.001$ by two-tailed Student's t-test. ## $p<0.01$ by Fisher exact probability test.

Figure 2. *Flt3*^{ITD} causes HSC depletion, HPC expansion and GMP expansion at, or shortly after, birth.

(A) Absolute HSC numbers in fetal or P0 livers for the indicated genotypes. (B) Absolute HSC numbers in P14 and adult bone marrow (2 hind limbs) or P14 spleen. (C, D) Fetal and adult HPC numbers (2 hind limbs). (E) GMP frequencies in fetal liver or adult bone marrow. (F) Liver or spleen weights. In all panels, error bars indicate standard deviations; n=6-20 biological replicates for each age and genotype. * $p<0.05$; ** $p<0.01$; *** $p<0.001$ by two-tailed Student's t-test relative to the wild type control at the same time point.

Figure 3. *Flt3*^{ITD} and *Runx1* mutations cooperate to deplete HSCs and expand committed progenitor populations after birth.

(A-D) HSC frequencies in E14.5 fetal liver, P0 liver, P14 bone marrow and P21 bone marrow for the indicated genotypes. (E-H) HPC frequencies in E14.5 fetal liver, P0 liver, P14 bone marrow and P21 bone marrow for the indicated genotypes. (I-L) GMP frequencies in E14.5 fetal liver, P0 liver, P14 bone marrow and P21 bone marrow for the indicated genotypes. (M, N) Percentages of CD45.2$^+$ donor leukocytes (M) or CD11b$^+$Gr1$^+$ myeloid cells (N) in the peripheral blood of recipients of P0 liver or P21 bone marrow cells from control or *Flt3*$^{ITD/+;}$ *Runx1*$^{\Delta/+}$ mice. Measurements are shown at 2 and 4 weeks after transplantation. (O, P) Percentage of recipients with multi-lineage (O) or myeloid (P) donor reconstitution at 4 weeks after transplantation. In all panels, error bars indicate standard deviations. For A-L, n=8-18 biological replicates per genotype and age. For M-P, n=14-15 recipients from 3 independent donors. Statistical significance was determined with a one-way ANOVA followed by Holm-Sidak's post-hoc test

for multiple comparisons (* p<0.05; ** p<0.01; *** p<0.001), or # p<0.0001 by the Fisher exact probability test.

Figure 4. FLT3^{ITD} activates STAT5 in both fetal and adult progenitors, but it activates the MAPK pathway after birth.

(A) Western blot showing phosphorylation of STAT5, ERK1/2, STAT3 and AKT in adult wild type and *Flt3*$^{ITD/+}$ HSC/MPPs, HPCs and GMPs. (B) *Flt3*$^{ITD/+}$*; Runx1*$^{\Delta/\Delta}$ progenitors give rise to AML in adult mice (right panel) that is not observed in wild type or *Flt3*$^{ITD/+}$ bone marrow. Scale bars indicate 100 microns. (C) STAT5 and MAPK are hyper-phosphorylated in *Flt3*$^{ITD/+}$*; Runx1*$^{\Delta/\Delta}$ AML that develops in adult mice. (D) STAT5 and ERK1/2 phosphorylation in wild type and *Flt3*$^{ITD/+}$ HSC/MPPs at E14.5, P0, P14 and adulthood. (E) STAT5 phosphorylation in wild type and *Flt3*$^{ITD/+}$ HPCs at E14.5, P0, P14 and adulthood. (F) ERK1/2 phosphorylation in wild type and *Flt3*$^{ITD/+}$ HPCs at E14.5, P0, P14 and adulthood. Each blot is representative of 2 (panels A and C) or at least 3 (panels D-F) independent experiments.

Figure 5. MAPK pathway inhibition does not prevent HSC depletion or committed progenitor expansion in *Flt3*$^{ITD/+}$ mice.

(A-D) HSC numbers (A), HPC numbers (B) and GMP frequencies (C) in wild type and *Flt3*$^{ITD/+}$ mice that were treated with vehicle or PD0325901 for 10 days beginning at 6 weeks after birth; n=4-5 biological replicates per genotype and treatment. (D-F) HSC numbers (D), HPC numbers (E) and GMP frequencies (F)

985 in P19 wild type, *Flt3*$^{ITD/+}$ and *Flt3*$^{ITD/ITD}$ mice whose mothers were given
986 PD0325901 beginning at P1; n=4-15 biological replicates for each genotype and
987 treatment. In all panels, error bars indicate standard deviation. Statistical
988 comparisons were made with a two-tailed Student's t-test. * p<0.05 relative to
989 vehicle treated cells with equivalent genotypes; # p<0.05 relative to similarly
990 treated wild type controls; ^ p<0.05 relative to similarly treated wild type and
991 *Flt3*$^{ITD/+}$ groups.
992
993 **Figure 6. *Stat5a/b* deletion exacerbates rather than rescues HSC depletion,**
994 **HPC expansion, GMP expansion and MPN in *Flt3*$^{ITD/+}$ mice.**
995 (A-D) HSC numbers (A), HPC numbers (B), GMP frequencies (C) and spleen
996 weights (D) in *Flt3*$^{ITD/+}$*; Stat5a/b*$^{f/f}$*; Mx1-Cre* compound mutant mice and littermate
997 controls; n=6-20 biological replicates per genotype. *Stat5a/b* was conditionally
998 deleted 6 weeks after birth, and this caused a complete loss of protein
999 expression (figure supplement 1). (E-H) HSC numbers (E), HPC numbers (F),
1000 GMP frequencies (G) and spleen weights (H) in *Flt3*$^{ITD/+}$*; Stat5a/b*$^{f/+}$*; Vav1-Cre*
1001 compound mutant mice and littermate controls; n=8-20 biological replicates per
1002 genotype. (I) The data suggest that STAT5-dependent pathways promote HSC
1003 self-renewal downstream of FLT3^{ITD}, but these effects are outweighed by STAT5-
1004 independent myeloid commitment pathways. In all panels, error bars indicate
1005 standard deviation. Statistical significance was determined with a one-way
1006 ANOVA followed by Holm-Sidak's post-hoc test for multiple comparisons.
1007 *p<0.05; ** p<0.01; *** p<0.001.

Figure 7. FLT3^{ITD} activates STAT5-dependent self-renewal programs and STAT5-independent commitment programs.

(A) Overview of experimental design. (B) Heatmap representing genes that were differentially expressed in *Flt3^{ITD}* mutant HPCs relative to wild type HPCs in both experiments 1 and 2. Each column represents an independent sample. The gene names and dendrogram are shown in figure supplement 1 attached to this figure. (C) Self-renewal and commitment-related gene sets were generated by identifying genes that were more highly expressed (>5 fold, adj. p<0.05) in HSCs relative to HPCs (self-renewal), or HPCs relative to HSCs (commitment). GSEA plots show ectopic activation of self-renewal-related genes in HPCs that express FLT3^{ITD}, but these effects are reversed in *Stat5a/b*-deficient HPCs. (D) An independently curated self-renewal gene set (Ivanova et al., 2002) was similarly enriched in wild type and *Flt3$^{ITD/+}$* HPCs relative to *Flt3$^{ITD/+}$; Stat5$^{\Delta/\Delta}$* HPCs. (E) GSEA revealed enrichment of gene sets associated with increased inflammatory cytokine signaling.

Figure 8. *Flt3^{ITD}*-mediated changes in gene expression correlate with the normal transition from fetal to adult transcriptional programs.

(A) Heatmap showing expression of FLT3^{ITD} target genes at E14.5, P0, P14 and adult stages. Each column shows average fold change in *Flt3$^{ITD/+}$* HPCs relative wild type HPCs at the indicated time point; n=3-4 independent arrays per genotype. The gene names and dendrogram are shown in figure supplement 1

attached to this figure. (B) Representative examples of expression of STAT5-independent (*Ctsg*) and STAT5-dependent (*Socs2*) $FLT3^{ITD}$ targets. Error bars reflect standard deviation. ***adj. p<0.05 relative to wild type at the same time point, # adj. p<0.05 relative to $Flt3^{ITD/+}$ at the same time point. (C) Heterochronic genes began transitioning from fetal to adult expression patterns between P0 and P14, concordant with sensitivity to $FLT3^{ITD}$. Genes that encode transcription factors and RNA binding proteins are noted to the right of the heatmap. A complete gene list is provided in source data table 1 attached to this figure. (D) Representative examples of heterochronic genes that show decreased (*Lin28b*) or increased (*Esr1*; Estrogen Receptor α) expression in adult relative to fetal HSCs and HPCs. Error bars reflect standard deviation. $$ adj. p<0.05 relative to E14.5 for both HSCs and HPCs. (E) Principal component analysis and Euclidean distance measurements show that gene expression in P0 HSCs more closely resembles fetal HSCs than adult HSCs, and gene expression in P14 HSCs more closely resembles that of adult HSCs. Similar calculations for HPCs are shown in figure supplement 2.

Figure 9. *$Flt3^{ITD}$* and *Runx1* mutations cooperatively induce changes in gene expression at P14, yet they have a much smaller effect at P0.

(A) Venn diagram showing overlap between genes that were significantly differentially expressed (adj. p<0.05, fold change ≥3) in *$Flt3^{ITD/+}$; $Runx1^{\Delta/+}$* HPCs relative to wild type at P14 or P0; n=4-5 arrays per genotype and age. (B) GSEA shows that differentially expressed genes in *$Flt3^{ITD/+}$; $Runx1^{\Delta/+}$* HPCs overlap

significantly with genes that are differentially expressed in *Flt3*$^{ITD/+}$*; Tet2*$^{\Delta/\Delta}$ HPCs (Shih et al., 2015). (C) Heatmap showing expression of genes that were differentially expressed in *Flt3*$^{ITD/+}$*; Runx1*$^{\Delta/+}$ HPCs relative to wild type HPCs. Each column indicates average fold change relative to the wild type samples from the same time point. The gene list is shown in source data table 1 attached to this figure. (D) Representative examples of genes that are among the most differentially expressed in *Flt3*$^{ITD/+}$*; Runx1*$^{\Delta/+}$ HPCs relative to wild type HPCs at P14. Most show much smaller changes in expression at P0. Error bars reflect standard deviations, * adj. p<0.05. (E) GSEA identified several gene sets that were enriched in *Flt3*$^{ITD/+}$*; Runx1*$^{\Delta/+}$ HPCs relative to wild type HPCs at P14. Three of the most significantly enriched gene sets are shown for P14 and P0.

Supplemental Figure Legends

Figure 4 – figure supplement 1. The PI3K/mTORC2 pathway does not mediate HSC depletion or MPN in *Flt3*^{ITD} mutant mice.

(A) Western blot showing STAT5 and AKT phosphorylation in wild type and *Flt3*$^{ITD/ITD}$ HPCs. *Pten*-deficient HPCs were included as a positive control for AKT phosphorylation. *Rictor* deletion prevented AKT hyper-phosphorylation by mTORC2. (B,C) HSC numbers in two tibias and femurs (B) and spleen weights (C) in *Flt3*$^{ITD/ITD}$*; Rictor*$^{f/f}$*; Vav1-Cre* compound mutant mice (and the indicated controls) after conditional *Rictor* deletion; n=3-12 per genotype. Error bars indicate standard deviations.

Figure 5 – figure supplement 1. Inhibition of the MAPK pathway fails to rescue FLT3^{ITD}-mediated HSC depletion and myeloid progenitor expansion, but *Stat5a/b* deletion enhances these phenotypes.

A Western blot was performed with 25,000 HPCs from wild type and *Flt3*$^{ITD/+}$, vehicle and PD0325901 treated mice. PD0325901 inhibited ERK1/2 phosphorylation without affecting STAT5 phosphorylation.

Figure 6 – figure supplement 1. *Stat5a/b* deletion causes a complete loss of phosphorylated and total STAT5 protein.

A Western blot was performed with 25,000 HPCs from wild type, *Flt3*$^{ITD/+}$ and *Flt3*$^{ITD/+}$*; Stat5*$^{\Delta/\Delta}$ adult mice (representative of 2 independent experiments). ERK1/2 phosphorylation was not affected by STAT5 deletion. STAT3 phosphorylation was not affected, and STAT1 and AKT phosphorylation were not detectable (not shown).

Figure 7 – figure supplement 1. FLT3^{ITD} induces STAT5-dependent and STAT5-independent changes in gene expression.

An expanded version of Figure 7B with the dendrogram and gene names attached to the heatmap.

Figure 8 – figure supplement 1. FLT3^{ITD}-mediated changes in gene expression correlate temporally with a transition from fetal to adult transcriptional states.

An expanded version of Figure 8A with the dendrogram and gene names attached to the heatmap.

Figure 8 – figure supplement 2. HPCs express heterochronic genes and begin to transition from fetal to adult transcriptional programs by P14.

Principal component analysis shows temporal changes in HPC gene expression before and after birth. Euclidean distance measurements and permutation testing show that P0 HPCs more closely resemble fetal HPCs than adult HPCs. P14 HPCs more closely resemble adult HPCs.

Source Data Tables

Figure 7 – source data table 1. Significantly differentially expressed genes in *Flt3*$^{ITD/+}$ HSCs and HPCs. Fold changes are shown for 270 probes that represent 254 differentially expressed genes in *Flt3*$^{ITD/+}$ HPCs relative to controls. HSC fold change data are also shown. P-values and adjusted p-values reflect significance across the entire time course.

Figure 7 – source data table 2. Self-renewal-related and commitment-related gene sets. These gene sets were determined by identifying genes that were more highly expressed in HSCs relative to HPCs (self-renewal) or HPCs relative to HSCs (commitment). In each case, a fold change threshold of 5 and an adjusted p-value threshold of <0.05 were used to define the lists.

Figure 8 – source data table 1. Heterochronic gene expression in wild type HSCs and HPCs. Source data (log2) are shown for the 250 most differentially expressed probes in developing HSCs (228 unique genes).

Figure 9 – source data table 1. *Flt3*^{ITD} and *Runx1* mutations cooperatively induce changes in gene expression in post-natal HPCs. Genes that are differentially expressed (Adjusted p<0.05, fold change ≥3) in *Flt3*$^{ITD/+}$*; Runx1*$^{\Delta/+}$ HPCs at P0 and P14 are shown in the indicated tables.

Figure 1

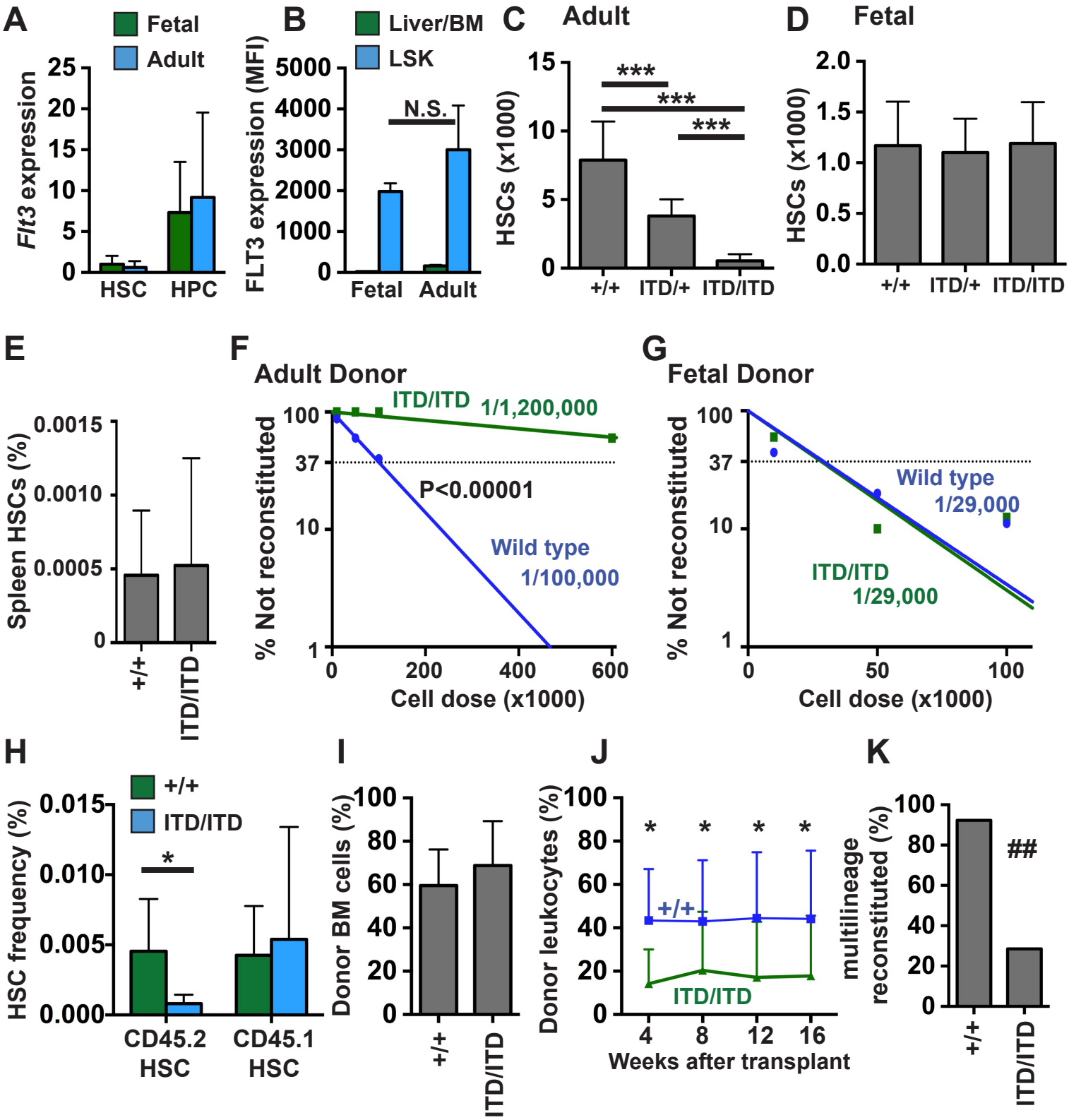
A
Fetal
Adult
Flt3 expression
25
20
15
10
5
0
HSC
HPC
B
Liver/BM
LSK
FLT3 expression (MFI)
5000
4000
3000
2000
1000
0
N.S.
Fetal
Adult
C
Adult
HSCs (x1000)
15
10
5
0
***
***
***
+/+
ITD/+
ITD/ITD
D
Fetal
HSCs (x1000)
2.0
1.5
1.0
0.5
0.0
+/+
ITD/+
ITD/ITD
E
Spleen HSCs (%)
0.0015
0.0010
0.0005
0
+/+
ITD/ITD
F
Adult Donor
% Not reconstituted
100
37
10
1
ITD/ITD
1/1,200,000
P<0.00001
Wild type
1/100,000
0
200
400
600
Cell dose (x1000)
G
Fetal Donor
% Not reconstituted
100
37
10
1
Wild type
1/29,000
ITD/ITD
1/29,000
0
50
100
Cell dose (x1000)
H
+/+
ITD/ITD
HSC frequency (%)
0.015
0.010
0.005
0.000
*
CD45.2
HSC
CD45.1
HSC
I
Donor BM cells (%)
100
80
60
40
20
0
+/+
ITD/ITD
J
Donor leukocytes (%)
100
80
60
40
20
0
* * * *
+/+
ITD/ITD
4
8
12
16
Weeks after transplant
K
multilineage reconstituted (%)
100
80
60
40
20
0
##
+/+
ITD/ITD

Figure 2

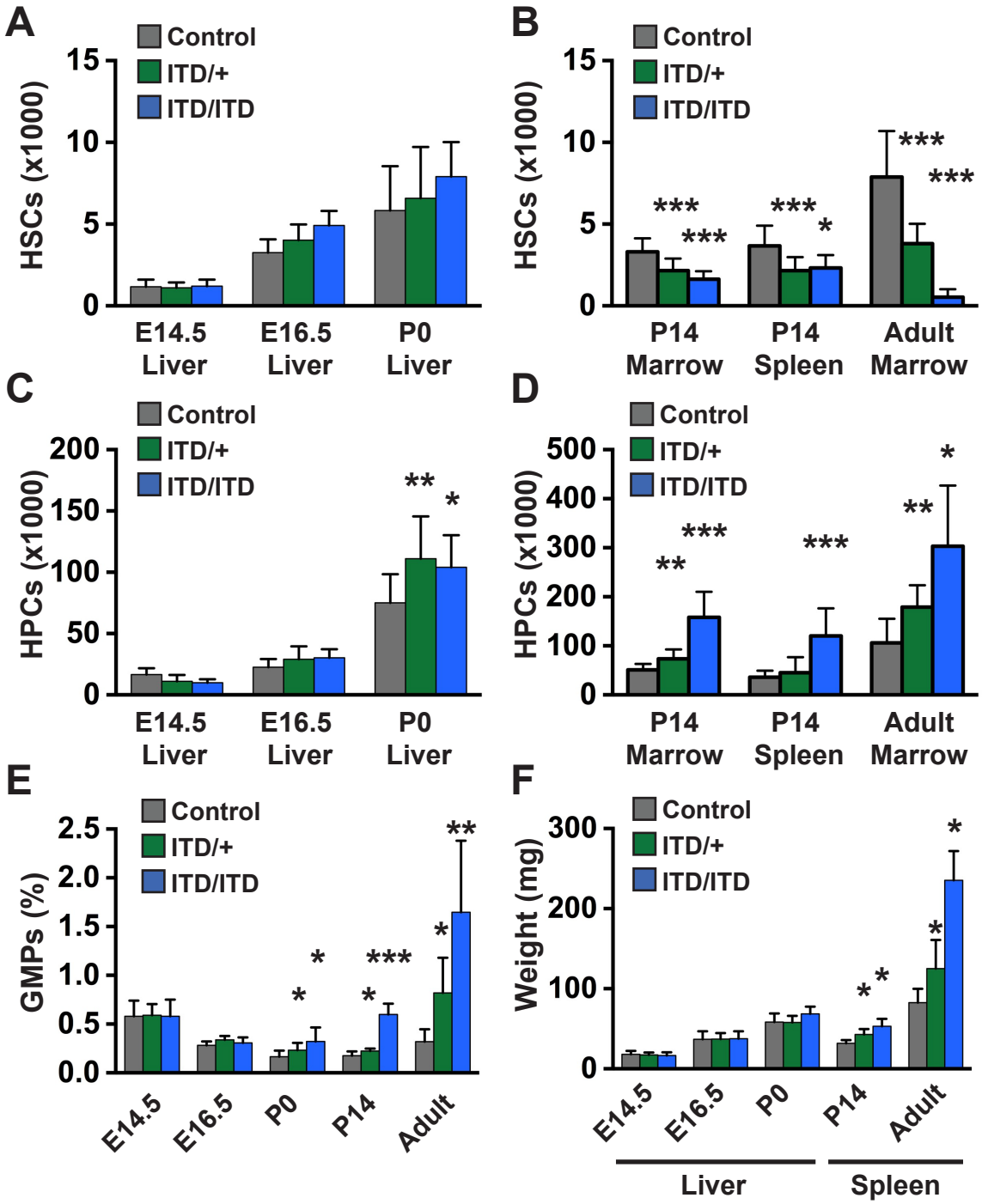
A
Control
ITD/+
ITD/ITD
HSCs (x1000)
15
10
5
0
E14.5 Liver
E16.5 Liver
P0 Liver
B
Control
ITD/+
ITD/ITD
HSCs (x1000)
15
10
5
0
***
***
***
***
*
***
***
P14 Marrow
P14 Spleen
Adult Marrow
C
Control
ITD/+
ITD/ITD
HPCs (x1000)
200
150
100
50
0
**
*
E14.5 Liver
E16.5 Liver
P0 Liver
D
Control
ITD/+
ITD/ITD
HPCs (x1000)
500
400
300
200
100
0
**
***
***
**
*
P14 Marrow
P14 Spleen
Adult Marrow
E
Control
ITD/+
ITD/ITD
GMPs (%)
2.5
2.0
1.5
1.0
0.5
0.0
*
*
*
***
*
**
E14.5
E16.5
P0
P14
Adult
F
Control
ITD/+
ITD/ITD
Weight (mg)
300
200
100
0
*
*
*
*
E14.5
E16.5
P0
P14
Adult
Liver
Spleen

Figure 3

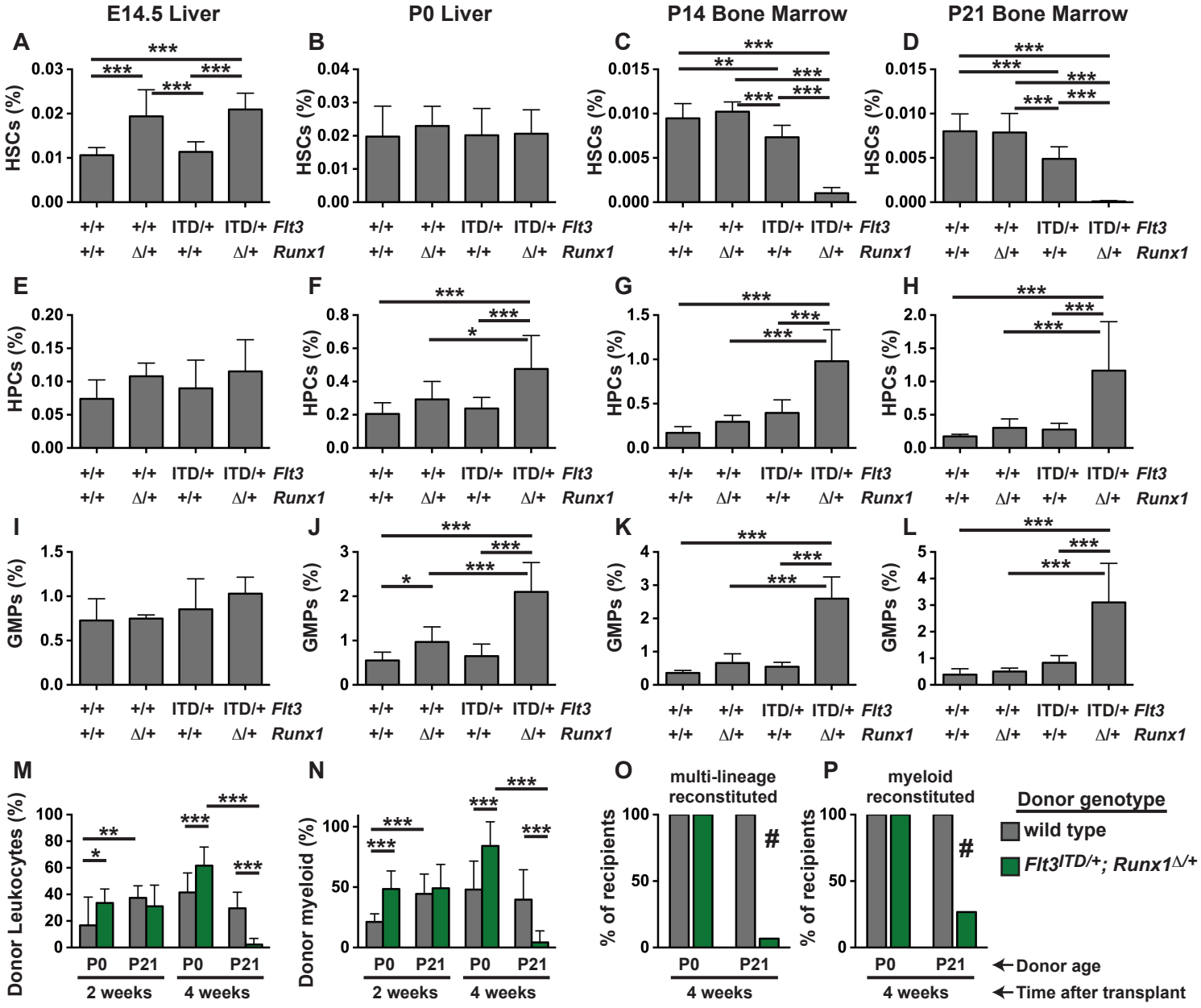
E14.5 Liver
P0 Liver
P14 Bone Marrow
P21 Bone Marrow
A
B
C
D
HSCs (%)
E
F
G
H
HPCs (%)
I
J
K
L
GMPs (%)
+/+ +/+ ITD/+ ITD/+ Flt3
+/+ Δ/+ +/+ Δ/+ Runx1
M
N
O
P
Donor Leukocytes (%)
Donor myeloid (%)
P0 P21 P0 P21
2 weeks 4 weeks
multi-lineage reconstituted
myeloid reconstituted
% of recipients
4 weeks
Donor genotype
wild type
Flt3ITD/+; Runx1Δ/+
Donor age
Time after transplant

Figure 4

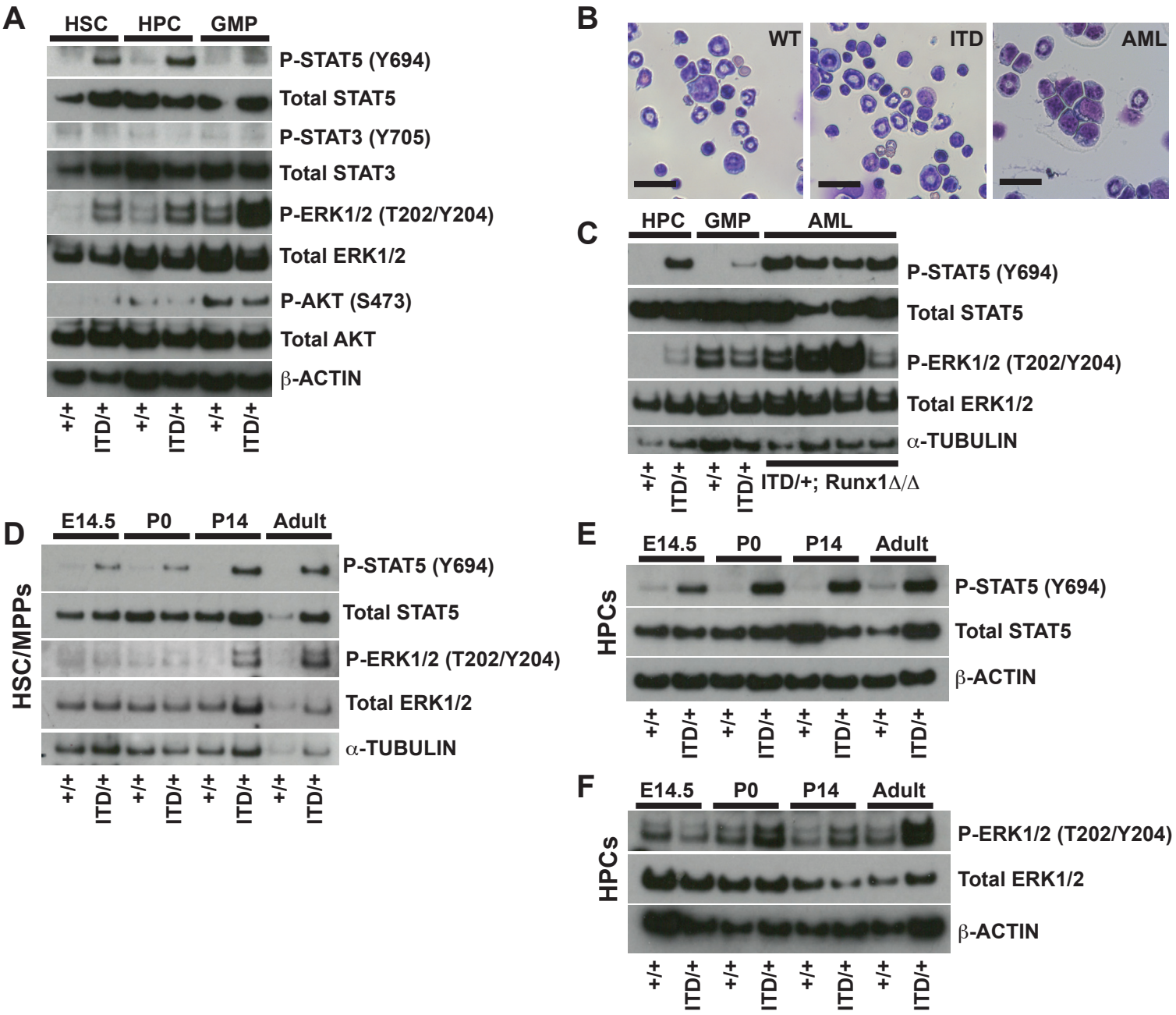
A
HSC
HPC
GMP
P-STAT5 (Y694)
Total STAT5
P-STAT3 (Y705)
Total STAT3
P-ERK1/2 (T202/Y204)
Total ERK1/2
P-AKT (S473)
Total AKT
β-ACTIN
+/+
ITD/+
B
WT
ITD
AML
C
HPC
GMP
AML
P-STAT5 (Y694)
Total STAT5
P-ERK1/2 (T202/Y204)
Total ERK1/2
α-TUBULIN
ITD/+; Runx1Δ/Δ
D
E14.5
P0
P14
Adult
HSC/MPPs
P-STAT5 (Y694)
Total STAT5
P-ERK1/2 (T202/Y204)
Total ERK1/2
α-TUBULIN
E
HPCs
P-STAT5 (Y694)
Total STAT5
β-ACTIN
F
HPCs
P-ERK1/2 (T202/Y204)
Total ERK1/2
β-ACTIN

Figure 5

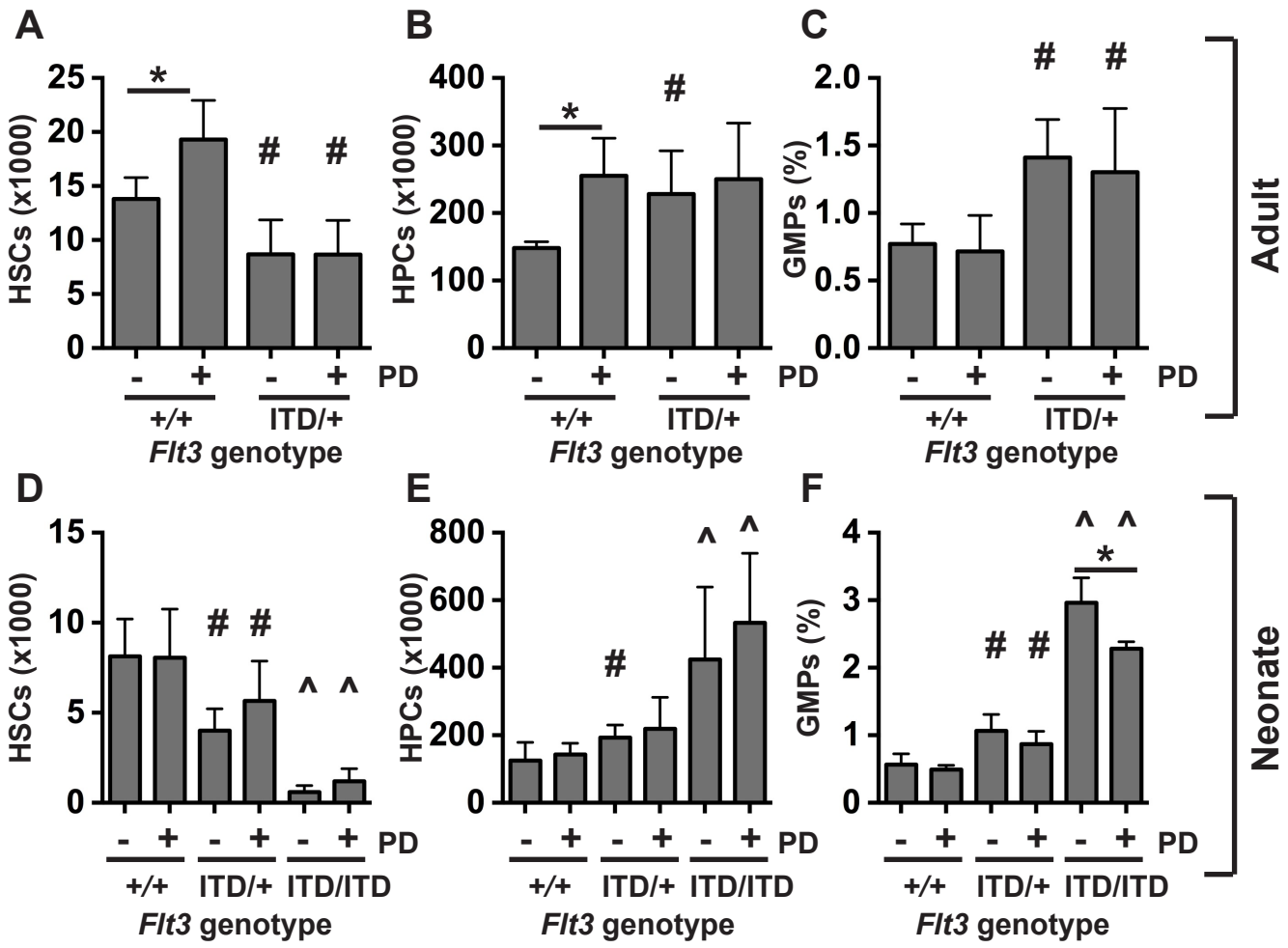
A
B
C
D
E
F
HSCs (x1000)
HPCs (x1000)
GMPs (%)
PD
+/+
ITD/+
ITD/ITD
Flt3 genotype
Adult
Neonate

Figure 6

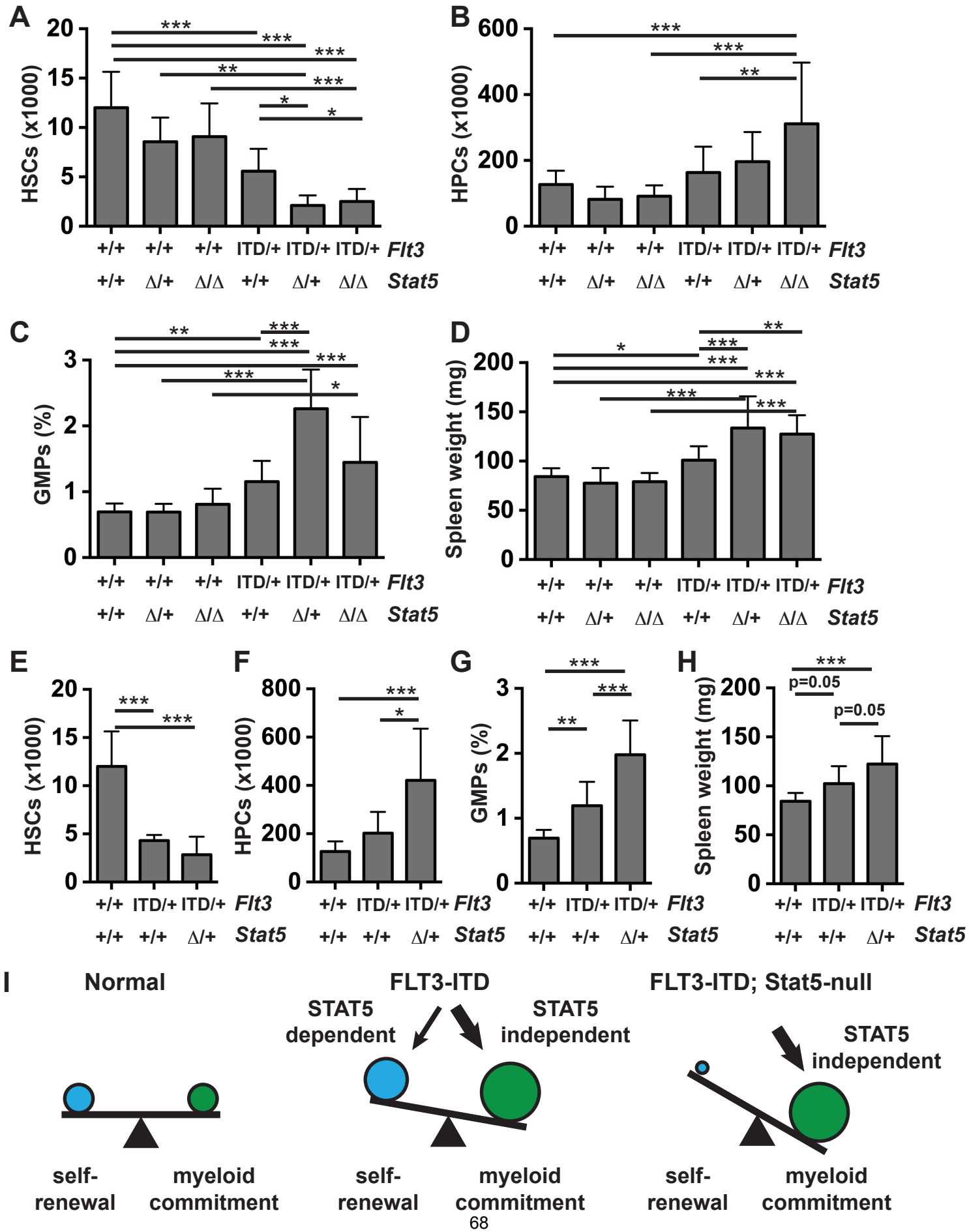
A
HSCs (x1000)
20
15
10
5
0
***
***
***
**
***
*
*
+/+ +/+ +/+ ITD/+ ITD/+ ITD/+ Flt3
+/+ Δ/+ Δ/Δ +/+ Δ/+ Δ/Δ Stat5
B
HPCs (x1000)
600
400
200
0
***
***
**
+/+ +/+ +/+ ITD/+ ITD/+ ITD/+ Flt3
+/+ Δ/+ Δ/Δ +/+ Δ/+ Δ/Δ Stat5
C
GMPs (%)
3
2
1
0
**
***
***
***
***
*
+/+ +/+ +/+ ITD/+ ITD/+ ITD/+ Flt3
+/+ Δ/+ Δ/Δ +/+ Δ/+ Δ/Δ Stat5
D
Spleen weight (mg)
200
150
100
50
0
*
**
***
***
***
***
***
+/+ +/+ +/+ ITD/+ ITD/+ ITD/+ Flt3
+/+ Δ/+ Δ/Δ +/+ Δ/+ Δ/Δ Stat5
E
HSCs (x1000)
20
15
10
5
0
***
***
+/+ ITD/+ ITD/+ Flt3
+/+ +/+ Δ/+ Stat5
F
HPCs (x1000)
800
600
400
200
0
***
*
+/+ ITD/+ ITD/+ Flt3
+/+ +/+ Δ/+ Stat5
G
GMPs (%)
3
2
1
0
***
***
**
+/+ ITD/+ ITD/+ Flt3
+/+ +/+ Δ/+ Stat5
H
Spleen weight (mg)
200
150
100
50
0
***
p=0.05
p=0.05
+/+ ITD/+ ITD/+ Flt3
+/+ +/+ Δ/+ Stat5
I
Normal
FLT3-ITD
FLT3-ITD; Stat5-null
STAT5 dependent
STAT5 independent
STAT5 independent
self-renewal
myeloid commitment
self-renewal
myeloid commitment
self-renewal
myeloid commitment

Figure 7

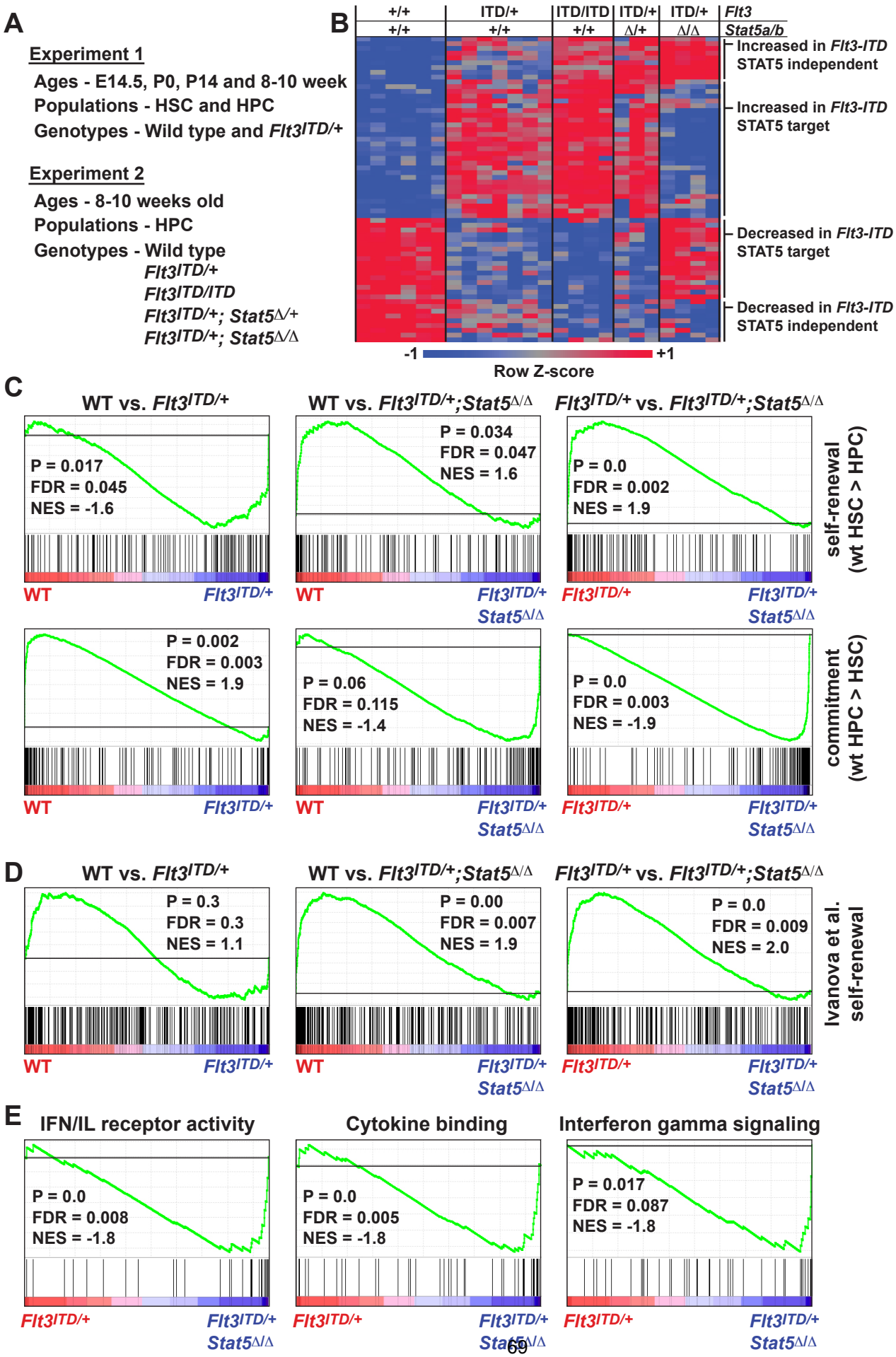
A
Experiment 1
Ages - E14.5, P0, P14 and 8-10 week
Populations - HSC and HPC
Genotypes - Wild type and Flt3ITD/+
Experiment 2
Ages - 8-10 weeks old
Populations - HPC
Genotypes - Wild type
Flt3ITD/+
Flt3ITD/ITD
Flt3ITD/+; Stat5Δ/+
Flt3ITD/+; Stat5Δ/Δ
B
+/+ +/+
ITD/+ +/+
ITD/ITD +/+
ITD/+ Δ/+
ITD/+ Δ/Δ
Flt3
Stat5a/b
Increased in Flt3-ITD STAT5 independent
Increased in Flt3-ITD STAT5 target
Decreased in Flt3-ITD STAT5 target
Decreased in Flt3-ITD STAT5 independent
-1
+1
Row Z-score
C
WT vs. Flt3ITD/+
WT vs. Flt3ITD/+;Stat5Δ/Δ
Flt3ITD/+ vs. Flt3ITD/+;Stat5Δ/Δ
P = 0.017
FDR = 0.045
NES = -1.6
P = 0.034
FDR = 0.047
NES = 1.6
P = 0.0
FDR = 0.002
NES = 1.9
self-renewal (wt HSC > HPC)
P = 0.002
FDR = 0.003
NES = 1.9
P = 0.06
FDR = 0.115
NES = -1.4
P = 0.0
FDR = 0.003
NES = -1.9
commitment (wt HPC > HSC)
WT
Flt3ITD/+
Flt3ITD/+
Stat5Δ/Δ
D
WT vs. Flt3ITD/+
WT vs. Flt3ITD/+;Stat5Δ/Δ
Flt3ITD/+ vs. Flt3ITD/+;Stat5Δ/Δ
P = 0.3
FDR = 0.3
NES = 1.1
P = 0.00
FDR = 0.007
NES = 1.9
P = 0.0
FDR = 0.009
NES = 2.0
Ivanova et al. self-renewal
WT
Flt3ITD/+
Flt3ITD/+
Stat5Δ/Δ
E
IFN/IL receptor activity
Cytokine binding
Interferon gamma signaling
P = 0.0
FDR = 0.008
NES = -1.8
P = 0.0
FDR = 0.005
NES = -1.8
P = 0.017
FDR = 0.087
NES = -1.8
Flt3ITD/+
Flt3ITD/+
Stat5Δ/Δ

Figure 8

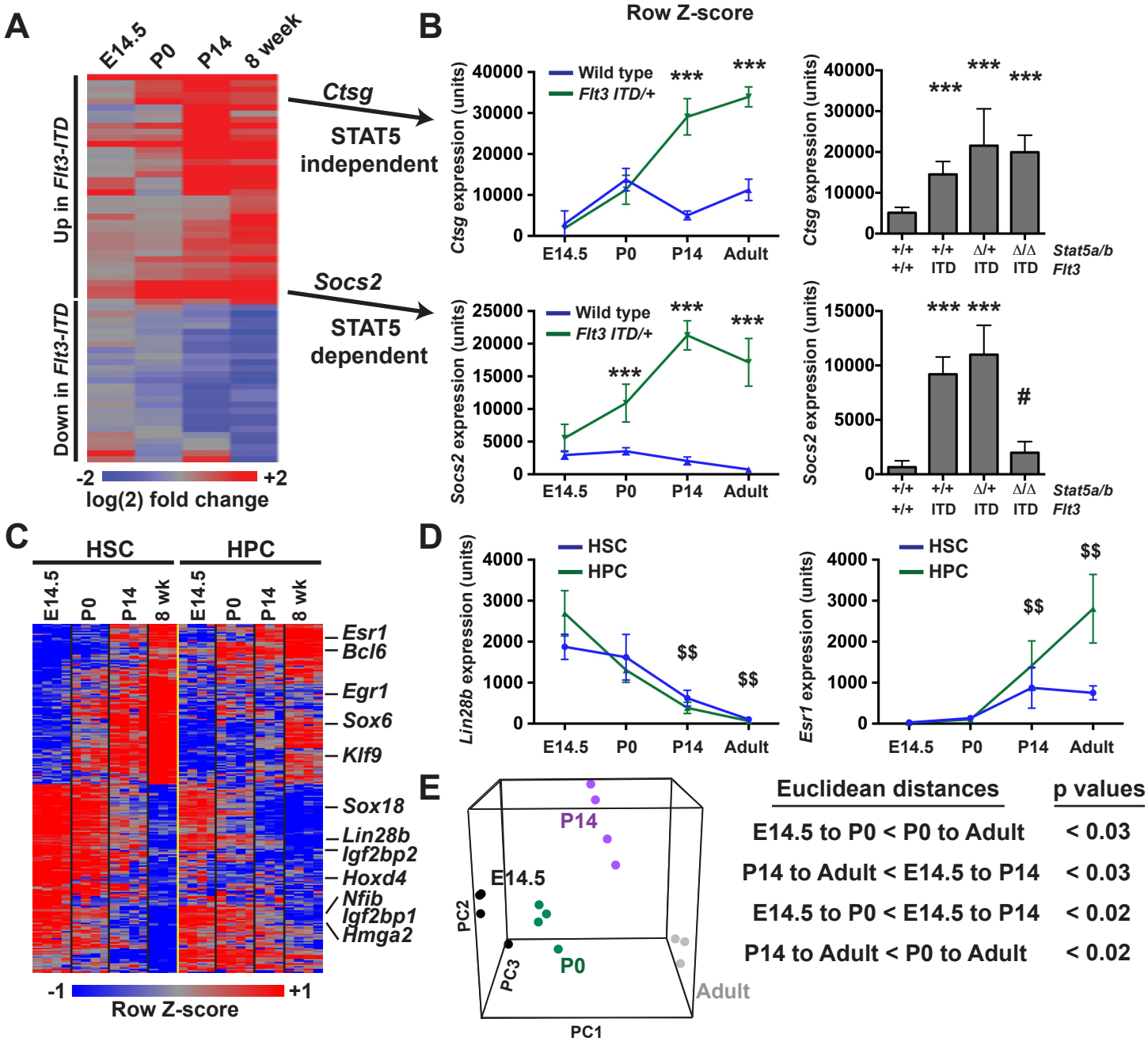
A
E14.5
P0
P14
8 week
Up in Flt3-ITD
Down in Flt3-ITD
Ctsg
STAT5 independent
Socs2
STAT5 dependent
-2
+2
log(2) fold change
B
Row Z-score
Wild type
Flt3 ITD/+
Ctsg expression (units)
Socs2 expression (units)
E14.5
P0
P14
Adult
+/+ +/+
+/+ ITD
Δ/+ ITD
Δ/Δ ITD
Stat5a/b Flt3
C
HSC
HPC
E14.5
P0
P14
8 wk
Esr1
Bcl6
Egr1
Sox6
Klf9
Sox18
Lin28b
Igf2bp2
Hoxd4
Nfib
Igf2bp1
Hmga2
-1
+1
Row Z-score
D
HSC
HPC
Lin28b expression (units)
Esr1 expression (units)
E
P14
E14.5
P0
Adult
PC1
PC2
PC3
Euclidean distances
p values
E14.5 to P0 < P0 to Adult
< 0.03
P14 to Adult < E14.5 to P14
< 0.03
E14.5 to P0 < E14.5 to P14
< 0.02
P14 to Adult < P0 to Adult
< 0.02

Figure 9

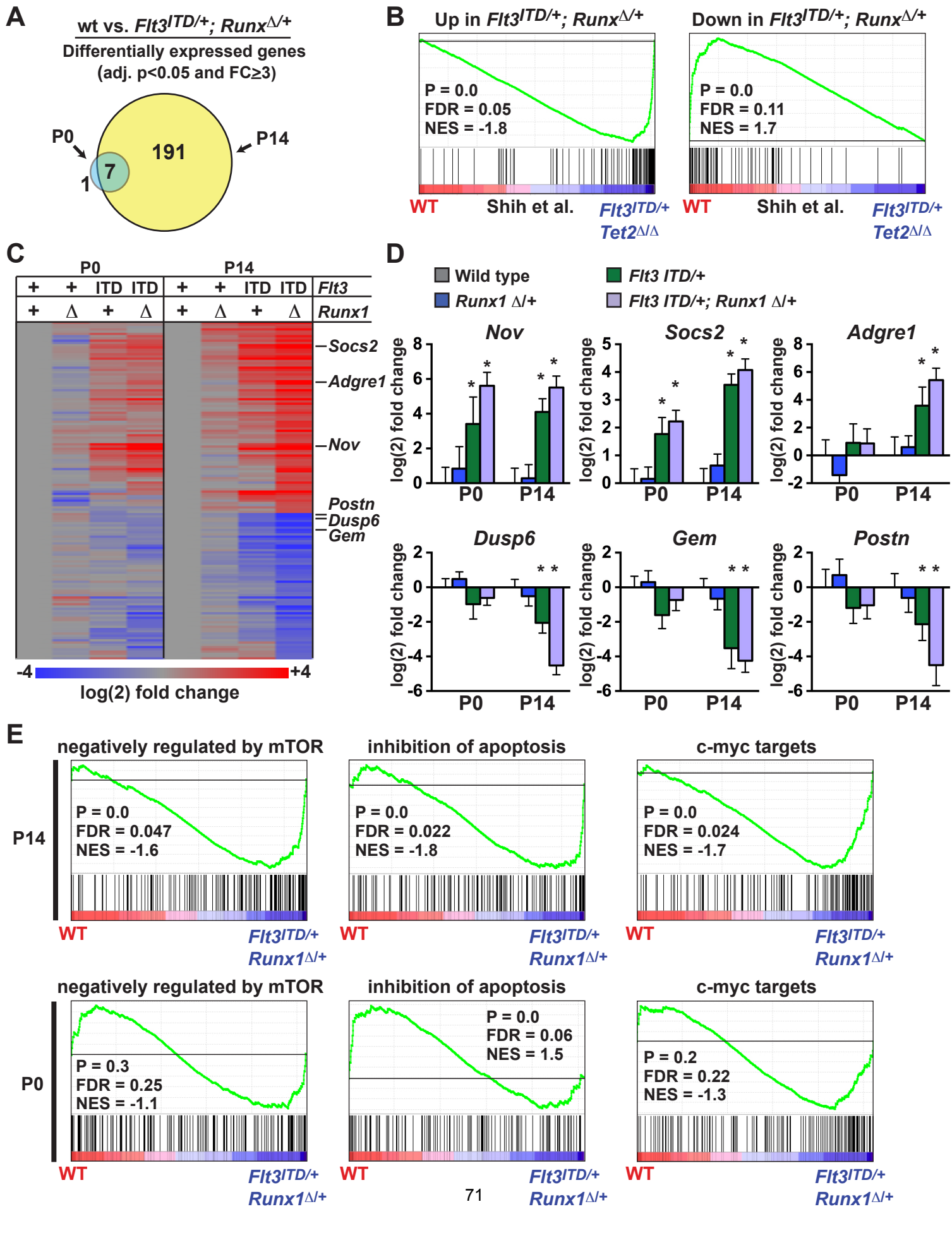
A
wt vs. Flt3ITD/+; RunxΔ/+
Differentially expressed genes
(adj. p<0.05 and FC≥3)
P0
P14
191
7
1
B
Up in Flt3ITD/+; RunxΔ/+
P = 0.0
FDR = 0.05
NES = -1.8
WT
Shih et al.
Flt3ITD/+ Tet2Δ/Δ
Down in Flt3ITD/+; RunxΔ/+
P = 0.0
FDR = 0.11
NES = 1.7
WT
Shih et al.
Flt3ITD/+ Tet2Δ/Δ
C
P0
P14
+ + ITD ITD + + ITD ITD Flt3
+ Δ + Δ + Δ + Δ Runx1
Socs2
Adgre1
Nov
Postn
Dusp6
Gem
-4
+4
log(2) fold change
D
Wild type
Flt3 ITD/+
Runx1 Δ/+
Flt3 ITD/+; Runx1 Δ/+
Nov
Socs2
Adgre1
Dusp6
Gem
Postn
log(2) fold change
P0
P14
E
negatively regulated by mTOR
inhibition of apoptosis
c-myc targets
P14
P = 0.0
FDR = 0.047
NES = -1.6
P = 0.0
FDR = 0.022
NES = -1.8
P = 0.0
FDR = 0.024
NES = -1.7
WT
Flt3ITD/+ Runx1Δ/+
P0
P = 0.3
FDR = 0.25
NES = -1.1
P = 0.0
FDR = 0.06
NES = 1.5
P = 0.2
FDR = 0.22
NES = -1.3

Figure 4 - figure supplement 1

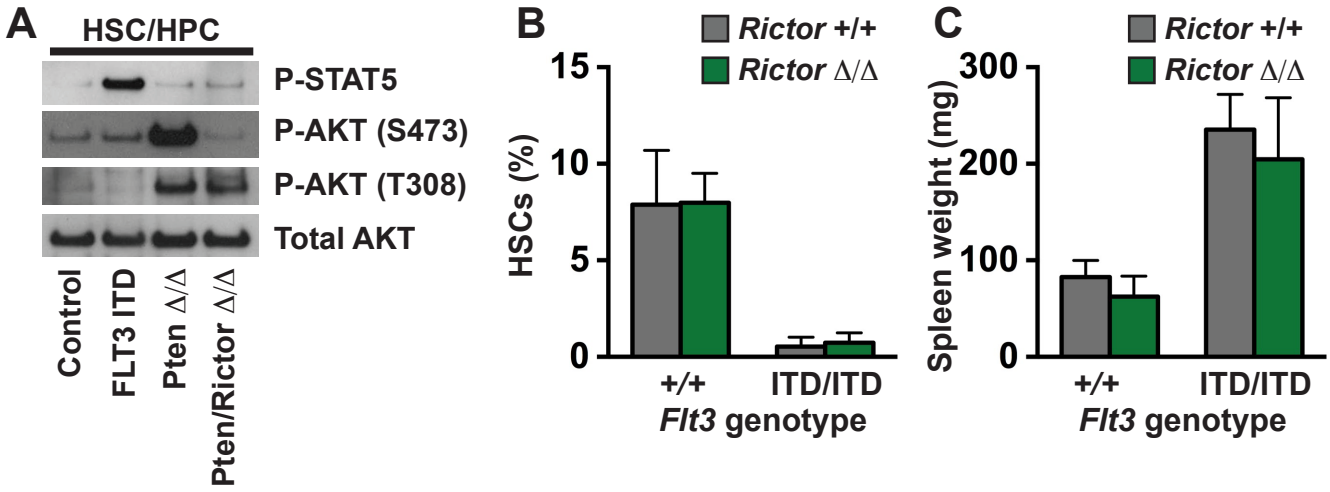

Figure 5 - figure supplement 1

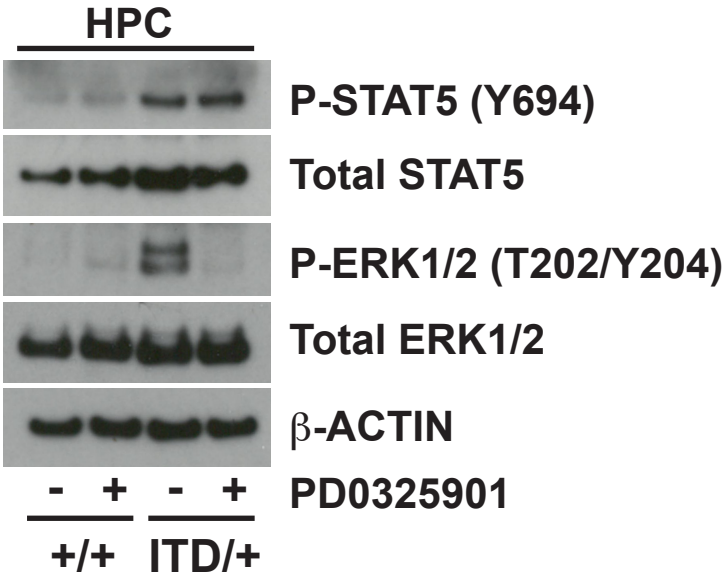

Figure 7 - figure supplement 1

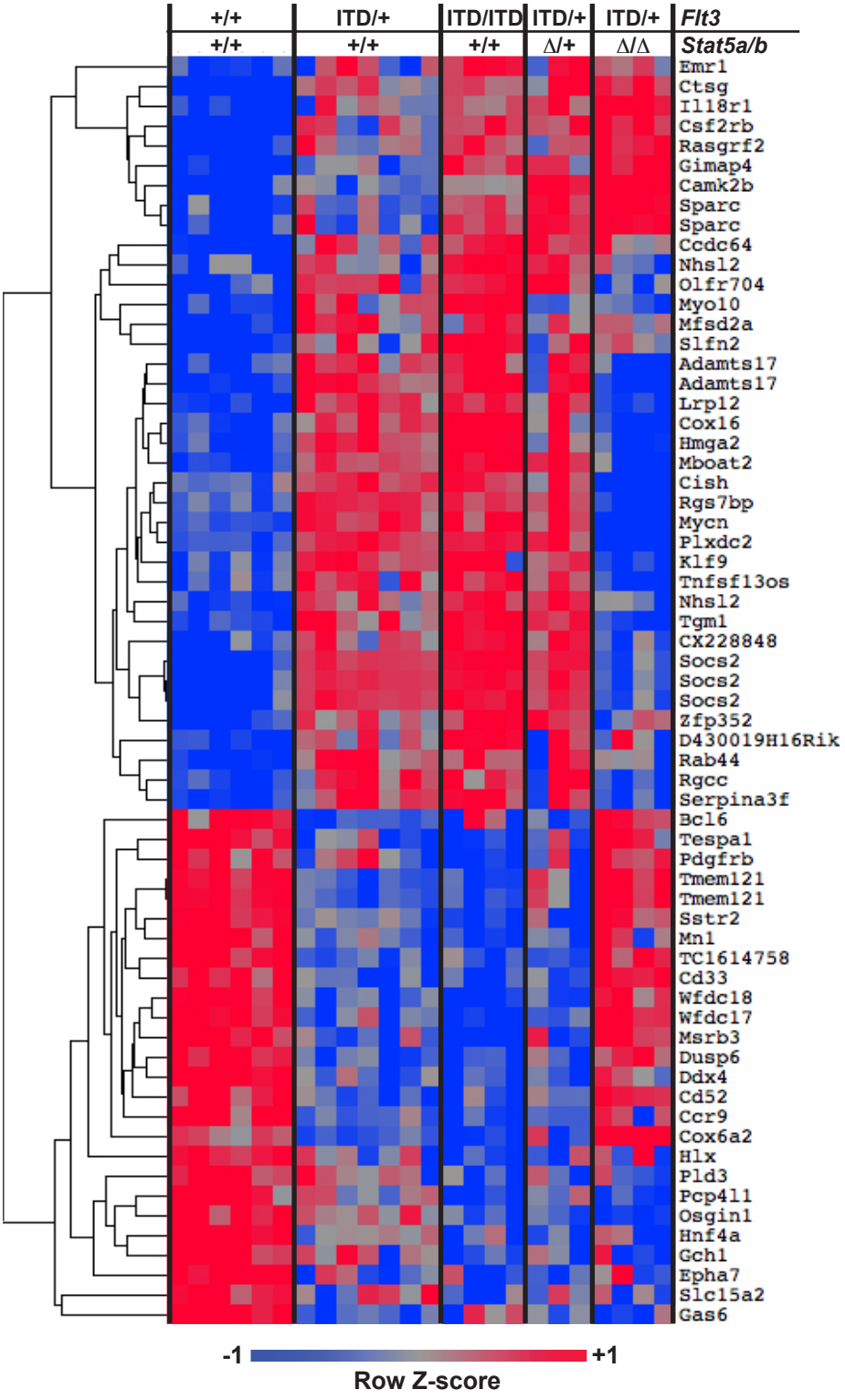

Figure 8 - figure supplement 1

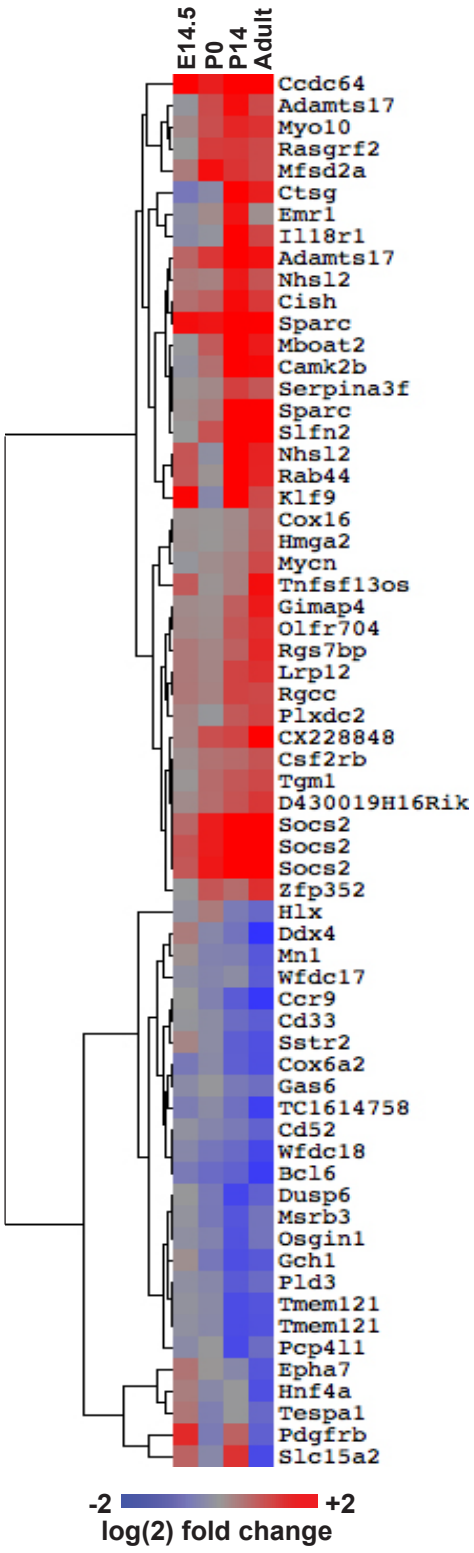

Figure 8 - figure supplement 2

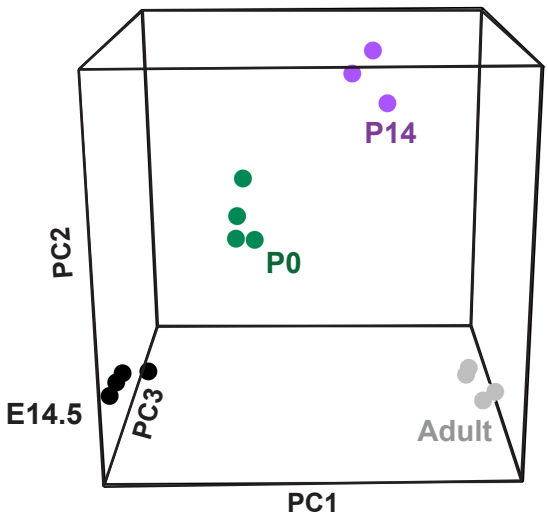

Euclidean distances	p values
E14.5 to P0 < P0 to Adult	< 0.02
P14 to Adult < E14.5 to P14	< 0.02
E14.5 to P0 < E14.5 to P14	< 0.03
P14 to Adult < P0 to Adult	< 0.03